Andreia De Rossi

DENSE AND POROUS GEOPOLYMERS DEVELOPED FROM INDUSTRIAL WASTES

Thesis presented to the Graduate Program in Chemical Engineering of the Federal University of Santa Catarina, as a requirement for obtaining the PhD degree in Chemical Engineering.

Advisors at UFSC
Regina F. P. M. Moreira
Dachamir Hotza

Supervisor at IPVC, Portugal
Manuel J. Ribeiro

Florianópolis
2019

Ficha de identificação da obra elaborada pelo autor através do Programa de Geração Automática da Biblioteca Universitária da UFSC.

De Rossi, Andreia
DENSE AND POROUS GEOPOLYMERS DEVELOPED FROM INDUSTRIAL WASTES / Andreia De Rossi ; orientadora, Regina de Fátima Peralta Muniz Moreira ; coorientador, Manuel J. Ribeiro 2019.

117 p.

Tese (doutorado) – Universidade Federal de Santa Catarina, Centro Tecnológico, Programa de Pós-Graduação em Engenharia Química, Florianópolis, 2019.

Inclui referências.

1. Engenharia Química. 2. aluminossilicatos. 3. geopolímeros. 4. resíduos. 5. porosidade. I. Moreira, Regina de Fátima Peralta Muniz. II. Ribeiro, Manoel J. III. Universidade Federal de Santa Catarina. Programa de Pós-Graduação em Engenharia Química. IV. Título.

Andreia De Rossi

DENSE AND POROUS GEOPOLYMER DEVELOPED FROM INDUSTRIAL WASTES

This thesis was presented to obtain the Title of PhD in Chemical Engineering and approved in its final version by the Graduate Program in Chemical Engineering of the Federal University of Santa Catarina.

Florianópolis, May 22, 2019.

_____
Prof. Cíntia Soares, Dr.ª
Program Coordinator

_____
Prof. Regina F.P.M. Moreira, Dr.ª
Advisor
Federal University of Santa Catarina

_____
Prof. Dachamir Hotza, Dr.
Co-Advisor
Federal University of Santa Catarina

_____
Prof. Manuel J. Ribeiro, Dr.
Co-Advisor, Polytechnic Institute of Viana do Castelo, Portugal

Examiners:

_____
Prof. Melissa G.A. Vieira, Dr.ª
State University of Campinas

_____
Prof. Michael Peterson, Dr.
Santa Catarina Extreme South University

_____
Cristiano José de Andrade, Dr.
Federal University of Santa Catarina

_____
Prof. Agenor De Noni Jr, Dr.
Federal University of Santa Catarina

This thesis is dedicated to my family, husband and friends for all love and help.

ACKNOWLEDGEMENTS

To God who enlightens and guides my life.

I would like to specially thank my advisor Dr.ª Regina de Fátima Peralta Muniz Moreira and my Co-Advisors Dr. Dachamir Hotza and Dr. Manuel J. Ribeiro, by the counsels and conversations, always receiving me with much affection and attention, giving me support so that the research was completed successfully.

I am grateful to my colleagues and supervisors (Cesarina de Freitas, Lisandro Simão, Prof. Dr. João Abrantes and Prof. Manuel Ribeiro) at Polytechnique Institute of Viana do Castelo (UIDM-ESTG), Portugal, for the valuable support provided during my doctoral internship as part of the activities of project CAPES/FCT 88887.125458/2016-00.

To colleagues of Ceramic e Composite Materials Research Laboratories by the partnership, support, and making the work environment a great place to be. To Laboratory of Glass-Ceramic Materials (VITROCER), in particular the Postdoctoral Elisangela Guzi for help and exchange of ideas. And I am grateful to the Laboratory of Energy and the Environment (LEMA-UFSC), for the valuable support for this research.

I would like to acknowledge Federal University of Santa Catarina (UFSC), in particular to those involved with the Graduate Program in Chemical Engineering (PósENQ), for the relevant support that was offered along the last years.

I would like to thank CNPq (National Council for Scientific and Technological Development) and CAPES (Coordination for the Improvement of Higher Education Personnel) for the scholarships.

I also acknowledge all Professors and colleagues that have taught me during the Ph.D. Thus, thank you to everyone who in one way or another contributed to this research.

My best friends, Camilla, Ellen, Jaqueline, Camila J. and Kamila that make my life happier and more enjoyable, I thank you for the support of the conversations and the unique and sincere friendships.

Special thanks to my incredible husband, Gilson. Thanks for being by my side all the time, sharing the experiences and supporting me when I needed.

Finally, my greatest gratitude to my parents and grandparents for the encouragement and help to achieve this achievement. To my brothers, for the friendship and support and to my nephews, for the joy and affection. Having you is a blessing from God.

"Have the courage to follow your heart and your intuition. They somehow already know what you really want to become."
(Steve Jobs)

ABSTRACT

Geopolymers are synthetic materials formed by the activation of solid particles, rich in silicon and aluminum, with alkaline solutions. Many industrial wastes present chemical composition potentially suitable for the geopolymerization process, allowing the complete reaction of the constituents and obtaining properties adjusted for various applications. Thus, this thesis aimed at the use of solid wastes, biomass fly ash and construction wastes, in the development of geopolymers. The industrial wastes used are suitable for the development of geopolymers, generating a saving of up to 75% in the consumption of metakaolin, reducing the environmental impact of the extraction of natural resources and the economic cost of the production of metakaolin and the destination of the waste in landfills. The different methods of curing and concentration of alkaline activators studied showed that curing under environmental conditions of geopolymers is an adequate option for use in the in-situ construction industry. The geopolymer mortars produced with construction and demolition waste as a fine aggregate presented superior mechanical properties compared to mortars produced with natural aggregate (sand). The use of a porogenic agent (H_2O_2) in the development of porous geopolymer mortars caused an increase of 85% in the moisture absorption and desorption capacity, being the highest value found in the literature for mortars. Finally, the addition of porogenic agent at different cure times showed that it is possible to produce faujasite and P zeolites in geopolymers using the hydrothermal cure at 60 °C. Most importantly, in this work eco-friendly geopolymers were developed with low energy and environmental costs associated with mechanical, physical and chemical properties suitable for their applications.

Keywords: aluminosilicates, geopolymers, residues, porosity, mortars, zeolites.

RESUMO

Os geopolímeros são materiais sintéticos formados pela ativação de partículas sólidas, ricas em silício e alumínio, com soluções alcalinas. Muitos resíduos industriais apresentam composição química potencialmente adequada ao processo de geopolimerização, permitindo a completa reação dos constituintes e obtenção de propriedades ajustadas para diversas aplicações. Assim, essa tese visou o uso de resíduos sólidos, cinzas volantes de biomassa e resíduos de construção, no desenvolvimento de geopolímeros. Os resíduos industriais utilizados são adequados para o desenvolvimento de geopolímeros, gerando uma economia de até 75% no consumo de metacaulim, reduzindo o impacto ambiental da extração de recursos naturais e o custo econômico da produção de metacaulim e a destinação do produto. resíduos em aterros. Os diferentes métodos de cura e concentração de ativadores alcalinos estudados mostraram que a cura sob condições ambientais de geopolímeros é uma opção adequada para uso na indústria de construção in situ. As argamassas geopoliméricas produzidas com resíduos de construção e demolição como agregados finos apresentaram propriedades mecânicas superiores às argamassas produzidas com agregado natural (areia). O uso de um agente porogênico (H_2O_2) no desenvolvimento de argamassas geopoliméricas porosas causou um aumento de 85% na capacidade de absorção e dessorção de umidade, sendo o maior valor encontrado na literatura para argamassas. Finalmente, a adição de agente porogênico em diferentes tempos de cura mostrou que é possível produzir zeólitas de faujasita e P em geopolímeros utilizando a cura hidrotérmica a 60 °C. Mais importante ainda, neste trabalho geopolímeros ecologicamente corretos foram desenvolvidos com baixos custos energéticos e ambientais associados às propriedades mecânicas, físicas e químicas adequadas para suas aplicações.

Palavras-chave: aluminossilicatos, geopolímeros, resíduos, porosidade, argamassas, zeólitas.

RESUMO ESTENDIDO

Introdução

Geopolímeros são materiais sintéticos formados por ativação de partículas sólidas, com alto teor de sílica e alumina, em meio alcalino. São constituídos por uma malha tridimensional em que os átomos de silício se alternam com os de alumínio em coordenação tetraédrica, compartilhando todos os átomos de oxigênio (Davidovits, 1991).

Os geopolímeros proporcionam desempenho comparável ao cimento Portland comum em muitas aplicações, como substituição de produtos cerâmicos, cimentos e concretos para a indústria de construção, proteção ao fogo de prédios e de túneis, remoção e imobilização de resíduos tóxicos e radioativos, entre outras aplicações de alta tecnologia (Davidovits, 1994; Fernández-Pereira et al., 2018; Maleki et al., 2019; Roviello et al., 2015; Siyal et al., 2018). Além disso, comparativamente ao cimento Portland, há redução significativa nas emissões de gases de efeito estufa durante seu processamento (Peter Duxson et al., 2007; Hassan et al., 2019; McLellan et al., 2011).

A principal fonte de aluminossilicatos usada na produção de geopolímeros é o metacaulim. Esse material vem sendo usado por sua melhor dissolução no meio alcalino, facilidade de controle da razão Si/Al e coloração branca (Hardjito and Rangan, 2005). Contudo, o metacaulim tem disponibilidade limitada, elevados custo e gasto energético, decorrentes do processo de calcinação. Dessa forma, o uso de resíduos industriais, como a cinza volante, na substituição do metacaulim, como fonte de aluminossilicatos é uma solução amigável do ponto de vista ambiental (Zhuang et al., 2016).

As cinzas volantes são materiais sólidos particulados submicrométricos que apresentam conteúdos elevados em sílica (SiO_2), alumina (Al_2O_3), e quantidades menores de outros óxidos, como hematita (Fe_2O_3), óxido de cálcio (CaO), óxido de potássio (K_2O), óxido de magnésio (MgO). Essa composição química das cinzas volantes pode variar de acordo com as características dos carvões ou biomassas queimados, sendo classificados pela norma ASTM C618. Têm despertado um crescente interesse para aplicação em geopolímeros por ser um subproduto resultante da queima de carvão ou biomassa com composição química e características físicas favoráveis (Nazari et al., 2012).

Outro material com potencial para valorização devido à elevada geração e taxas de reciclagem baixas são os resíduos da construção e demolição (*Construction and Demolition Wastes*, CDW). Portanto a incorporação desse material na produção de argamassas de alvenaria

implica em uma alternativa de reciclagem de CDW no setor de construção civil (Saiz Martínez et al., 2016), com ampla utilização e redução do impacto ambiental gerado pela disposição final inadequada desses resíduos (Vásquez et al., 2016). Os CDW têm sido empregados por vários pesquisadores como agregado reciclado na produção de argamassas de alvenaria e os resultados encontrados mostram diminuição das propriedades mecânicas das argamassas (Jiménez et al., 2013; Ledesma et al., 2015; Martínez et al., 2013; Saiz Martínez et al., 2016). No entanto, não foram encontradas pesquisas que abordassem a utilização dos CDW como agregados finos para produção de argamassas geopoliméricas.

Diversos estudos disponíveis na literatura contemplam o uso de cinzas como ligantes para o processo de geopolimerização. Contudo, o uso de cinza de biomassa como ligante e resíduos da construção e demolição como agregado fino no desenvolvimento de pastas e argamassas tem sido pouco explorado.

Objetivos

O objetivo principal dessa tese consiste na avaliação do uso de cinza de biomassa e resíduos da construção e demolição na produção de geopolímeros densos e porosos. Adicionalmente, avaliaram-se os efeitos dos métodos de cura e da concentração dos ativadores alcalinos; da substituição do agregado natural pelo agregado reciclado em argamassas densas; da adição do agente porogênico em argamassas porosas aplicadas ao controle de umidade; e da cura hidrotermal em geopolímeros densos e porosos, nas características dos geopolímeros produzidos.

Metodologia

Para o desenvolvimento das pastas e argamassas geopoliméricas densas e porosas, foram selecionados dois resíduos industriais, cinzas de biomassa (*biomass fly ash*, BA) e o resíduo da construção e demolição (CDW). A BA e o metacaulim (MK) foram utilizados como fontes de aluminossilicatos, com proporção de 75% em massa de BA e 25% em massa de MK. A BA foi obtida a partir da queima de biomassa em caldeira de leito fluidizado de uma indústria de pasta de papel em Portugal e o MK, Argical M1200S, um silicato de alumínio comercial (Univar). O CDW foi utilizado como agregado fino no desenvolvimento de argamassas geopoliméricas.

O processo de geopolimerização foi realizado com a mistura de silicato de sódio e hidróxido de sódio (NaOH), ativadores alcalinos, nas proporções de 1,0 e 1,5 em massa. A solução de NaOH (10 M) foi preparada por dissolução de esferas de hidróxido de sódio em água

destilada. Como agente porogênico, foi utilizado peróxido de hidrogênio (H_2O_2) em diferentes concentrações (0,15, 0,30 e 0,45% em massa).

As variáveis estudadas no capítulo 2 foram os efeitos dos métodos de cura e ativadores alcalinos sobre as propriedades das pastas geopoliméricas. No capítulo 3, foram avaliadas as propriedades das argamassas geopoliméricas densas no estado fresco e endurecido, desenvolvidas com CDW e areia como agregado fino. No capítulo 4, argamassas geopoliméricas porosas foram desenvolvidas para o controle de umidade, de acordo com a norma ISO 24353 (2008). Para finalizar, no capítulo 5 foi avaliado o desenvolvimento de zeólitas em pastas geopoliméricas densas e porosas curadas em condições hidrotérmicas a 60 °C.

Para avaliar os materiais utilizados e as propriedades dos geopolímeros desenvolvidos, análises físicas, químicas, mineralógicas e microestruturais foram realizadas. Dentre essas análises, estão difração e fluorescência de raio X, microscopia eletrônica de varredura com espectroscopia de dispersão de raio X, resistência mecânica a compressão e flexão, termogravimetria e térmica diferencial, condutividade térmica, absorção de água, densidade aparente, porosidade, tamanho de partícula, entre outras análises específicas para cada capítulo experimental.

Resultados e Discussão

A cinza volante de biomassa, utilizada como ligante, é adequada para o desenvolvimento de geopolímeros, gerando uma economia de até 75% no consumo de metacaulim, reduzindo o impacto ambiental da extração de recursos naturais e o custo econômico da produção de metacaulim e da destinação dos resíduos em aterros sanitários.

Os diferentes métodos de cura e concentração de ativadores alcalinos estudados mostraram que a cura dos geopolímeros em condições ambientais é adequada para sua utilização *in-situ* na indústria da construção civil. Por outro lado, os demais métodos podem ser utilizados de acordo com as características e aplicações desejadas. As argamassas geopoliméricas produzidas com resíduos da construção, com a função de agregado fino, apresentaram propriedades mecânicas superiores em comparação às argamassas produzidas com agregado natural (areia) em todos os tamanhos de partícula estudados. Os maiores valores de resistência mecânica ($\backsim$40 MPa) foram obtidas com partículas na faixa de 0,5 e 2,0 mm.

A adição de H_2O_2 nas argamassas geopoliméricas ocasionou um aumento de 85% na capacidade de absorção e dessorção de umidade, indicando excepcional capacidade de tamponamento de umidade. Por

fim, a adição de agente porogênico e diferentes tempos de cura mostraram que é possível produzir materiais híbridos de zeólitas P/geopolímero e faujasita/geopolímero utilizando-se a cura hidrotérmica a 60 °C.

Conclusões finais

A combinação da BA e do CDW é apropriada para o desenvolvimento de geopolímeros. Os resultados obtidos neste estudo mostraram a possibilidade de produzir geopolímeros ecologicamente corretos com baixos custos energéticos e ambientais associados a propriedades mecânicas, físicas e químicas adequadas para as aplicações requeridas. As principais conclusões deste trabalho são:

- obtenção de geopolímeros baseados em BA com cura em condições ambientais,
- aumento nas propriedades mecânicas das argamassas ao substituir o agregado natural pelo agregado reciclado,
- alta capacidade de tamponamento de umidade com argamassas geopoliméricas porosas, e
- obtenção de zeólitas a partir da cura hidrotérmica de geopolímeros baseados em cinza de biomassa.

Palavras-chave: aluminossilicatos, geopolímeros, resíduos, porosidade, argamassas, zeólitas.

LIST OF FIGURES

LIST OF TABLES

LIST OF ABBREVIATIONS

ABNT	Brazilian Association of Technical Standards
AP	Apparent Porosity
BA	Biomass fly ash
BD	Bulk Density
BET	Brunauer–Emmer–Teller
CDW	Construction and Demolition Waste
CS	Compressive Strength
EDS	Energy Dispersive X-ray Spectroscopy
FS	Flexural Strength
FT	Flow Table
HC	Cure in Hydrothermal condition
MBV	Moisture Buffer Value
MK	Metakaolin
MIP	Mercury Intrusion Porosimetry
OPC	Ordinary Portland Cement
PO	Total Porosity
RC	Cure in Room condition
RH	Relative Humidity
SC	Cure in Water submerged condition
SEM	Scanning Electron Microscopy
SH	Sodium Hydroxide
SS	Sodium Silicate
SS:SH	Sodium Silicate: Sodium Hydroxide
TA	Thermal conductivity
TC	Cure in Thermal condition
STA (TG-DTA)	Simultaneous Thermal Analysis
UC	Cure in Usually condition
WA	Water Absorption
XRD	X-Ray Diffraction
XRF	X-Ray Fluorescence

TABLE OF CONTENTS

1. INTRODUCTION

Civil construction is one of the most demanded industrial activities in the world and it is becoming one of the sectors with the greatest impact on the economic development of the countries (Vásquez et al., 2016). The construction industry is responsible for 50% of the consumption of natural resources (European Commission, 2001) and for the generation of 5-7% of the global anthropogenic emissions of CO_2 during the production of the Ordinary Portland Cement (OPC) (Huntzinger and Eatmon, 2009; Meyer, 2009), motivating a constant concern related to the preservation of the environment.

Thus, the search for alternative materials to OPC and other natural raw materials is permanent. An alternative cementitious binder, denominated "geopolymer", is considered as a substitute for OPC (Turner and Collins, 2013), due to the high performance and structural and functional applications in multiple areas (Davidovits and Quentin, 1991).

Geopolymers consist of a Si-O-Al polymer structure, with alternately bonded SiO_4 and AlO_4 tetrahedra sharing all the oxygen atoms. Aluminum (Al^{3+}) and silicon (Si^{4+}) assume coordination 4 with oxygen (O^{2-}), that is, each one is connected to 4 oxygen atoms arranged at the vertices of an imaginary tetrahedron, which causes a negative charge imbalance. The electrical neutrality of the matrix is ensured by the presence of cations such as K^+, Na^+ and Ca^{2+} (Swanepoel and Strydom, 2002).

These cations are inserted into the polymeric structure of the hydration reaction of aluminosilicates through alkaline activation with alkaline or alkaline-earth solutions. Generally, alkaline hydroxide solutions (single activators) or a mixture of silicate and alkali hydroxide solutions (compound activators) are used as activators (Weng and Sagoe-Crentsil, 2007). The most commonly used simple activators are sodium hydroxide (NaOH) and potassium (KOH), with sodium silicate (Na_2xSiO_2+x or $(Na_2O)x \cdot SiO_2$) being the most frequently used compound activator (Pacheco-Torgal et al., 2008). Various grades of sodium silicate are available in the market, which are identified by their SiO_2:Na_2O weight ratio ranging from 2:1 to 3.75:1 (Lagaly et al., 2000).

The choice of materials for geopolymerization depends on factors such as availability, cost and type of application. Various inorganic materials have in their composition silica and alumina that can be alkali-activated (Pacheco-Torgal et al., 2008). Among the main materials that have been studied as raw materials for geopolymerization are metakaolin (Ahn et al., 2019; Zheng et al., 2019) and various industrial wastes such

as fly ash (De Rossi et al., 2019; Gunasekara et al., 2019; Lee et al., 2016; Liu et al., 2016b; Zhuang et al., 2016), waste glass (Bai et al., 2019; Toniolo et al., 2018) blast furnace slag (Collins and Sanjayan, 2002; Wang et al., 2015), red mud (Hertel et al., 2019; Novais et al., 2019; Toniolo et al., 2018) and mixtures of these materials (Cheng and Chiu, 2003; Koshy et al., 2019; Puertas and Fernández-Jiménez, 2003).

Due to the increasing cost of raw materials and the continuous reduction of natural resources, the selection of sustainable aluminosilicate materials has become imperative (Liguori et al., 2017) and new waste materials have been proposed according to the availability of each country/region where the geopolymers are being developed. Biomass ashes and construction and demolition waste present high generation and few recovery alternatives. Biomass ashes are chemically and physically similar to metakaolin and can substitute and maintain geopolymer characteristics with lower economic and environmental costs. Construction and demolition wastes have the potential to substitute metakaolin and natural aggregates for the development of mortars and concretes geopolymer.

Biomass ash is a waste generated through the thermal recovery by biomass combustion. In the paper and pulp industries, biomass ash is one of the main waste generated, since a large fraction of the forest biomass received is not suitable for the production of paper and cellulose, thus the biomass is valued through the generation of energy in the boilers (Al-Kassir et al., 2010; González et al., 2011; Haykırı-Açma, 2003; Sami et al., 2001).

Biomass combustion ash is classified as solid waste according to the European Waste List (European Commission, 2000), which is generally disposed of in landfills. However, landfilling is not sustainable, with economic and environmental disadvantages (Tarelho et al., 2015).

Ashes produced from biomass burning in boilers are classified as inert waste, Class II-B, according to the ABNT:NBR 10004 (2004) standard. It is a very variable residual material in composition, collected from both the bottom (bottom ash) and the particulate collection precipitator (fly ash) (FOELKEL, 2011). Global production of bottom ash and fly ash from biomass combustion is estimated at 480 Mtons/year (Modolo et al., 2014; Vassilev et al., 2013).

Considering the increasing amounts of biomass ash produced and associated environmental issues, many studies have evaluated the use of these ashes to develop environmentally friendly and sustainable building materials. Due to the physical characteristics, such as lower density and higher specific surface area, and chemical as high amounts of SiO_2 in

amorphous form, fly ash is more suitable for the development of geopolymers as compared to bottom ash (Loo and Koppejan, 2008; Tarelho et al., 2011; Vassilev et al., 2010).

Construction and demolition waste (CDW) has been identified by the European Commission as a priority stream because of the large amount of waste generated and its high potential for reuse and recycling (Vieira and Pereira, 2015). In Brazil, approximately 84 million m^3 of CDW were generated in 2014 (Miranda et al., 2016), and this amount continues to increase, motivating the constant search for new environmentally correct ways of use and/or disposal of these materials at a global level.

The incorrect allocation of CDW has caused flooding, loss of drainage infrastructure due to clogging of galleries, pollution and increased public administration costs. One way to reduce these negative impacts is by recycling CDW (Abrecon, 2015).

In order to regulate the management of CDW, a Brazilian ministerial resolution (CONAMA, 2002) defines that large public and private generators are obliged to develop and implement a management plan that aims at the reuse, recycling or other environmentally correct destination of CDW. Thus, for environmental and economic reasons there is a growing need for recycling. In addition, the scientific community, companies and the public sector have carried out several actions to develop this activity (Miranda et al., 2009).

Therefore, the recycling of CDW through geopolymerization is a topic of great interest because its use reduces the environmental impact generated by the inadequate disposal of these wastes and allows a wide use of waste (Vásquez et al., 2016). However, in this work CDW will not be used as a binder in the production of geopolymers, due to the economic cost associated with waste comminution. Nevertheless, CDW was applied as fine aggregates in the production of dense and porous geopolymer mortars.

In this work, thus, geopolymer materials were developed with biomass ash from the pulp and paper industry and with construction and demolition waste. The effects of the curing methods and the alkaline activator concentration on the physical and chemical properties of geopolymers were initially evaluated. In the sequence, the influence of the total substitution of the natural aggregate by the recycled aggregate (CDW) on the production of dense geopolymer mortars was studied. Next, the properties of porous geopolymer mortars for the control of humidity in built environments were investigated. Finally, geopolymers

with specific characteristics for the adsorption of liquid and gaseous pollutants were developed.

1.1. OBJECTIVES

1.1.1. General objective

The general objective of this work is the valorization of biomass ashes and construction and demolition waste in the development of dense and porous geopolymer materials for structural and environmental applications.

1.1.2. Specific objectives

The specific objectives of this thesis are:

- To characterize wastes through physical and chemical analysis and evaluate their potential in the development of geopolymers;
- To develop formulations based on the potentialities identified in the wastes for the development of dense and porous geopolymers;
- To characterize the physical, chemical and mineralogical properties of geopolymers in order to identify potential applications;
- To study the influence of the curing methods and the weight ratios of the activators on the characteristics of the geopolymers;
- To evaluate the porous geopolymers developed in the passive control of relative humidity of indoor built environments;
- To analyze the influence of particle size of the recycled fine aggregates on the fresh and hardened properties of dense geopolymer mortars;
- To produce zeolites in dense and porous geopolymer slides from biomass ash in hydrothermal conditions.

1.2. CONTENT OF THE THESIS

This thesis was proposed in the scope of the project “Development of low energy geopolymer hydraulic coatings from industrial solid waste for application in the passive control of built environments” of the CAPES/FCT program with international cooperation between the Federal

University of Santa Catarina (UFSC) and the Polytechnic Institute of Viana do Castelo (IPVC), Portugal.

The work was designed for recovery of waste from the pulp and construction industry for the manufacture of non-limestone hydraulic binders (geopolymers). Thus, in this thesis the focus was to use biomass fly ash from the paper industry as well as construction and demolition waste for the development of dense and porous geopolymer materials for different applications. This thesis is divided into 6 chapters, as described below. Chapters 2 to 5 contain the relevant state of art, experimental section, results, discussion and remarks.

- Chapter 1 provides a general introduction to the subject discussed in this thesis, the general and the specific objectives;

- Chapter 2 presents different curing methods and weight ratios of alkaline activators in the development of geopolymers, and their physical, chemical and mechanical properties;

- In Chapter 3, dense geopolymer mortars were developed with total replacement of the natural aggregate by the recycled aggregate. CDW was used as a fine aggregate, in three particle sizes, and the influence on the characteristics of the mortars in the fresh and hardened state were studied;

- In Chapter 4, the moisture control with porous geopolymer mortars was studied. H_2O_2 was used as a porogenic agent and CDW as a fine aggregate. The moisture adsorption and desorption cycles were performed in a climatic chamber;

- Chapter 5 was to evaluate the effect of hydrothermal conditions over time on the mineralogical characteristics of the geopolymer. The development of zeolites at different times and additions of H_2O_2 was evaluated and applications were suggested;

- In Chapter 6, the conclusions are summarized, as well as some suggestions for future work.

1.3. GENERAL METHODOLOGY

The structure of the experimental section of this thesis is divided into 4 chapters, (2 to 5), including processing and characterization methods carried out in each chapter, which are presented in the diagram in Figure 1. Specific procedures and analyzes are presented in each chapter. Generic methods are presented in the following sections.

1.3.1.Materials and processing

In this thesis, all geopolymers were prepared using a standard mixture of biomass ash (BA) and metakaolin (MK, Argical M 1200 S, Univar, Portugal) as a source of reactive silica and alumina (binder). BA provided the main aluminosilicate source (75 wt.%), whereas MK was used in lower content (25 wt.%). BA was obtained from biomass burning in a bubbling fluidized combustor of a paper pulp plant in Portugal.

For the development of dense and porous mortars, the construction and demolition wastes (CDW) were used as fine aggregates in different fractions, specific in the referential chapters. CDW was collected from a demolition site of a concrete-based construction and classified as 17.01.01 (concrete) and 17.01.02 (bricks) according to the European List of Wastes (EU, 2014). CDW was first segregated from wood residues, plastic and metals, and after was drying at 110 °C for 24 h. A double comminution process was then carried out: jaw crushing (BB2 Retsch) followed by hammer milling (5657 Retsch), to obtain particles ≤ 4 mm in diameter. The different fractions of CDW used for mortar development were selected by sieving.

A mixture of sodium silicate (SS, 9.13 wt.% Na_2O, 28.77 wt.% SiO_2, 62.1 wt.% H_2O; Quimiamel) and sodium hydroxide (SH, 97 wt.% purity, Sigma Aldrich) were used as alkaline activators with weight ratio SS:SH = 1.0 and/or SS:SH = 1.5. A NaOH solution (10 M) was prepared by dissolution of sodium hydroxide beads in distilled water.

The specific preparation of geopolymers is described in each experimental chapter.

Figure 1. Schematic diagram of the experimental section of this thesis. Abbreviations are referred to in the aforementioned list and in sections 1.3.1. and 1.3.2.

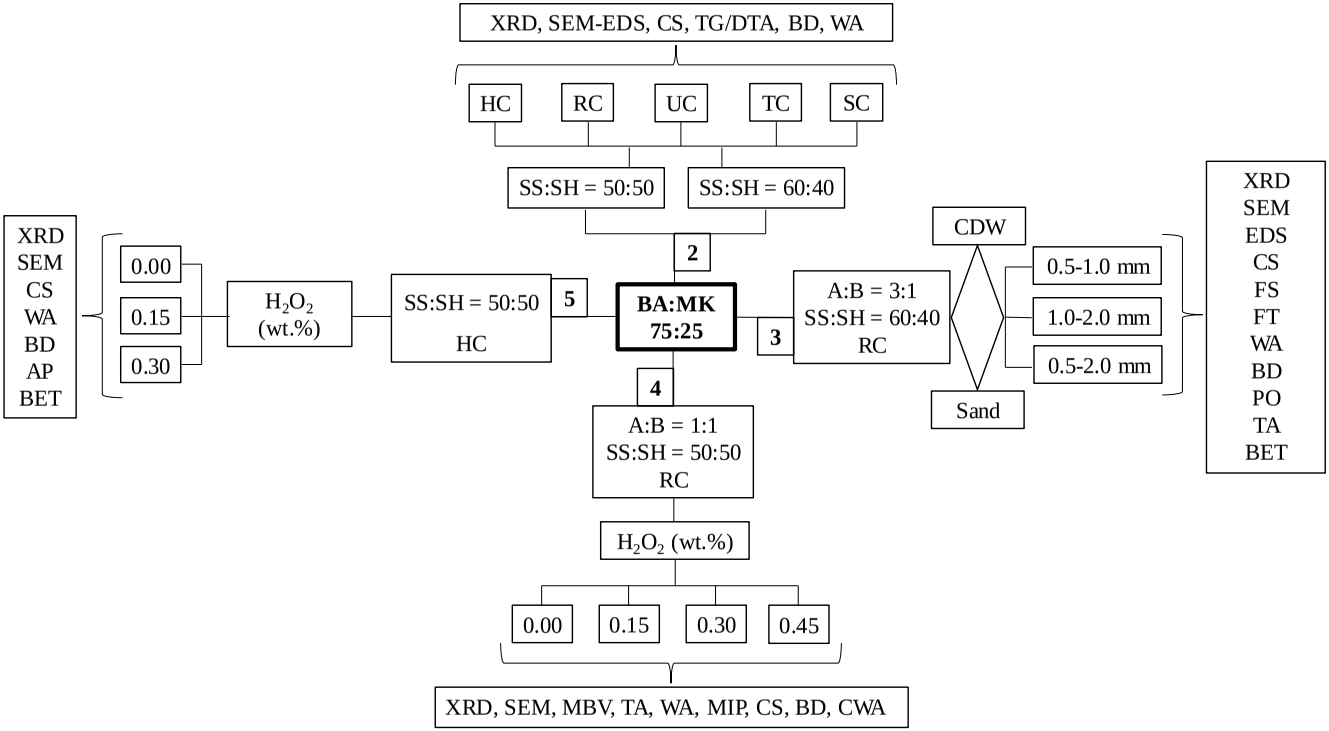

1.3.2. Characterization methods

For the characterization of raw materials and developed geopolymers physical, chemical, microstructural and mineralogical analyzes were performed. The analyzes performed in each experimental section are presented in the flowchart of Figure 1 and are described in this section. The specific methods for each geopolymer material are described in their respective chapters.

The mineralogical compositions of MK, BA, CDW and all geopolymers were evaluated by X-ray diffraction (XRD, D8 Advance Bruker) using Cu K α radiation, in the range of 5-80°, with a 0.02° step-scan and 10 s/step. Diffraction patterns were analyzed with the aid of ICDD database (International Center of Diffraction Data, PDF 4) in a dedicated software (EVA, Bruker). The chemical compositions of raw materials were obtained by X-ray fluorescence (XRF, X'Pert PRO MPD Philips), while the loss on ignition (LOI) at 1000 °C was also determined.

The particle size distribution (PSD) of BA was measured by laser scaterring (Malvern Mastersizer 3000). Microstructural analysis of BA and geopolymer was performed by scanning electron microscopy (SEM, SU1510, Hitachi) equipped with energy dispersion spectroscopy (EDS, Bruker).

Geopolymers, BA and MK were submitted to simultaneous thermal analysis, thermogravimetry/differential thermal analysis (TG/DTA, 402 EP, Netzsch) with a heating rate of 10 °C/min from 25-1000 °C. The thermal conductivity (TH) (ASTM C518, 2010) and water absorption coefficient (NP EN 1015-18) were measured using three cubic specimens (40 × 40 × 40 mm^3) of each formulation.

Physical characteristics of the geopolymers, such as water absorption (WA – Eq.1), bulk density (BD - Eq.2) and apparent porosity (AP - Eq.3), were estimated accordance to NBR 9778 (ANBT NBR 9778, 1987) and ASTM 373 (ASTM C373-88, 1999).

$$WA = \left[\frac{(M-D)}{D}\right] \times 100 \quad (1)$$

$$BD = \frac{D}{(M-S)} \quad (2)$$

$$AP = \left(\frac{M-D}{M-S}\right) \times 100 \quad (3)$$

Where M = saturated mass, D = dry mass and S = suspended mass.

For the dense geopolymer mortars, the compressive and flexural strength (CS and FS) measurements were performed according to EN 1015-11 (1999) from samples obtained by filling prismatic molds with the mortar, after compaction by manual vibration. The prismatic samples were removed from the molds after 24 h and subsequently cured in room conditions (20 °C and 68% relative humidity) for 28 days. A universal testing machine (Lloyd, LR 30 K) was used, running at a displacement rate of 0.5 mm/min. Three prismatic samples (40 × 40 × 160 mm^3) were tested for the flexural strength, resulting into 2 broken parts, which, according to the standard procedure, were then cut into 5 cubic samples (40 × 40 × 40 mm^3) for the compressive strength determinations (RAEIS SAMIEI et al., 2015). Average and standard deviation data were reported.

For paste and porous geopolymer mortars, the compressive strength (CS) was determined using a universal testing machine (LR 30 K, Lloyd) running at a displacement rate of 0.5 mm/min. Five cylindrical samples, which were polished flat, of each formulation (22 mm diameter × 44 mm length) were tested and the average data were reported.

The Brunauer–Emmer–Teller (BET) surface area and pore properties for geopolymers were measured by a N_2 adsorption–desorption isotherm at liquid nitrogen temperature (Gemini V2, Micromeritics Instrument Corporation, Norcross, GA), with N_2 as adsorbate after drying of the monolith samples (~ 0.1 mg) at 200 °C. Mercury intrusion porosimetry (MIP) was conducted using a porosimeter (Autopore IV 9500, Micromeritics Instrument Corp., Norcross, GA). Single-intrusion data were measured to provide information on the total porosity and the pore size.

2. EFFECT OF CURING METHODS AND ALKALINE ACTIVATORS RATIO INFLUENCE ON MICROSTRUCTURE AND PROPERTIES OF BIOMASS ASH GEOPOLYMERS[1]

In this Chapter, it is reported the effect of different curing conditions on the properties of geopolymers produced from biomass ash. Five different curing methods, moisture range, temperature control, concentration of alkali activators, and Na_2SiO_3/NaOH ratio were evaluated and their effect on the geopolymers are discussed.

Geopolymers are synthetic materials obtained by the alkaline activation of some materials rich in silicon and aluminum, mainly metakaolin and specific industrial wastes as fly ash and slag (Davidovits, 2008; Lee et al., 2019).

It is well-known that the geopolymers properties can be influenced by several factors, such as composition, material sources, water content, particle size, setting time and curing temperature (Zribi et al., 2019). All these variables can result in a wide range of properties and characteristics, including high compressive strength, low shrinkage, fast or slow setting, acid and fire resistance and low thermal conductivity (P. Duxson et al., 2007).

Compositionally, the geopolymers may be formulated according to the relative ratios between the major constituents, such as Al_2O_3, SiO_2, Na_2O and H_2O. The relationship between these oxides has been deeply discussed in the literature (Davidovits, 2008), offering a compositional support to predict specific properties. The increase of SiO_2/Al_2O_3 ratio enhances mechanical properties, and its control has been applied in studies where the geopolymers are intended for building and construction materials (Duxson et al., 2005; Ozer and Soyer-Uzun, 2015).

Another important factor for adjusting mechanical properties is the solid/liquid ratio (Lahoti et al., 2017), because the excess water during cure is adverse to the generated porosity (Xie and Kayali, 2014). Furthermore, it is necessary to better understand the processing conditions effects on the geopolymers properties, while achieving desired properties, and simultaneously reducing production costs and minimizing environmental impacts.

In general, fly-ash based geopolymer curing requires a thermal treatment that increases the manufacturing cost and the carbon footprint (Dong et al., 2017). However, heat curing improves geopolymerization,

[1] Submitted for publication.

and subsequently the mechanical behavior of final products. At room temperature, fly ash is not completely dissolved and the low reactivity increases the setting time of the geopolymer, affecting the mechanical properties (Dong et al., 2017).

Longer heat curing and higher temperatures can increase the strength of fly ash-based geopolymers at early ages (Adam and Horianto, 2014; Collins and Sanjayan, 2002; Mustafa Al Bakri et al., 2012; Puertas et al., 2000), but it leads to a lower strength at later ages. This is due to the fast reaction rate, which causes microstructural inhomogeneity, once the reaction products are located near porous structures. These reaction products form a barrier for further reaction, resulting in slow strength growth at later ages (Bakharev et al., 1999). In addition, fly ash-based geopolymers present highly stable structures when compared to metakaolin-based geopolymers (Kong et al., 2008). Therefore, to maintain acceptable early age strength, accelerate curing methods are normally be used.

According to Izquierdo et al. (Izquierdo et al., 2010), the curing conditions of fly ash/slag-based geopolymers affect the mechanical properties. Open cure conditions enable water to evaporate and, as a consequence, produce geopolymers with high porosity and low compressive strength. In contrast, protected curing promotes the binder development, giving rise to systems of lower porosity and higher mechanical resistance. Furthermore, the application of the obtained geopolymers is directly linked to the cure conditions (Izquierdo et al., 2010).

This work studies the influence of different curing treatments on the final characteristics of geopolymers, thus trying to better understand the phenomena involved during geopolymer processing. In this sense, physical and chemical properties as well as compressive strength at 28 days were measured. Moreover, the structure and morphology of geopolymers were analyzed by thermal gravimetric analysis (TGA), X-ray diffractometry (XRD), scanning electron microscopy (SEM), and energy-dispersive X-ray spectroscopy (EDS).

2.1. EXPERIMENTAL

The quantities (in a weight basis) and molar ratios of oxides present in the initial geopolymer paste are shown in Table 1.

Table 1. Geopolymer composition with two different sodium silicate (SS) to sodium hydroxide (SH) weight ratios.

Raw material (wt.%)	**SS:SH weight ratio**	
	1.0	**1.5**
BA	37.5	37.5
MK	12.5	12.5
SS	25	30
SH	25	20
Molar ratio		
SiO_2/Al_2O_3	4.54	4.79

Mixing of the geopolymer raw materials was performed in a planetary mixer (Kenwood), following the steps: i) previous homogenization of sodium silicate and NaOH solution at 60 rpm for 5 min; ii) mixture at the same speed of the alkaline solution with BA and MK for 10 min, and iii) mixture of the paste for further 5 min at 95 rpm.

Then, the paste was transferred to cylindrical plastic moulds and exposed to five methods of cure: Thermal Conditions (TC), Hydrothermal Conditions (HC), Room Conditions (RC), Water Submerged Conditions (SC) and Usual Conditions (UC), according to Figure 2.

In TC, the samples were kept in the hot chamber for 28 days at 40 °C. In HC, the samples were cured for 28 days in a hermetic bottle at 40 °C. In RC, the specimens remained in an open vessel at room temperature and humidity for 28 days (20 °C and 65%). In SC, the specimens were cured for 1 day at room temperature and humidity and after maintained for 27 days at 20 °C submerged in water. The UC method is a combination of methods TC and RC, traditionally employed in several works of the literature (Novais et al., 2018a, 2018b, 2016a, 2016b), which consists in curing the sealed samples for 24 h at 40 °C in a hot chamber (such as TC, but only for 1 day) and subsequently in open conditions at room temperature and humidity, during 27 days (similar to RC).

Figure 2. Geopolymers preparation and curing methods used. TC: Thermal Conditions; HC: Hydrothermal Conditions; RC: Room Conditions; SC: Submerged Conditions; UC: Usually Conditions.

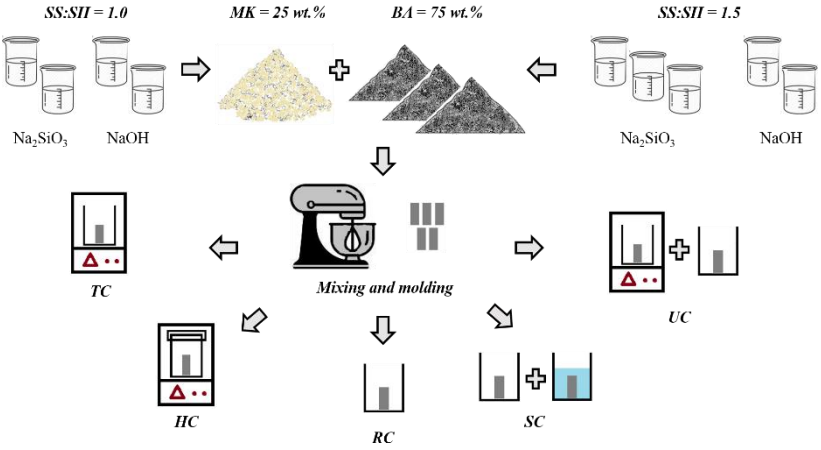

2.2. RESULTS

2.2.1.Raw materials characterization

Figure 3 shows the main chemical and mineral components of BA and MK. As reported in previous studies (De Rossi et al., 2019, 2018), the biomass fly ash consists of SiO_2 (34.0 wt.%), Al_2O_3 (13.5 wt.%), CaO (16.5 wt.%), K_2O (5.5 wt.%), MgO (3.1 wt.%), Na_2O (1.5 wt.%), Fe_2O_3 (5.0 wt.%), others (6.5 wt.%) and loss on ignition (LOI, 14.3 wt.%). MK is composed by SiO_2 (54.4 wt.%), Al_2O_3 (39.4 wt.%), others (3.08 wt.%) and LOI (2.66 wt.%). The main oxides present in BA were SiO_2, CaO and Al_2O_3, and those values are similar to the compositions of other biomass ashes available in the literature (Teixeira et al., 2019). For MK, the expected main presence of SiO_2 and Al_2O_3 was detected. The identified crystalline phases in BA were calcite, quartz and muscovite, while in MK, quartz and anatase were identified.

Figure 3. XRD patterns and main oxides (XRF) of BA and MK, where (Q = Quartz (PDF-00-046-1045); M = Muscovite (PDF-00-05-2035); A = Anatase (PDF-01-084-1285; Ca = Calcite (PDF-04-012-0489).

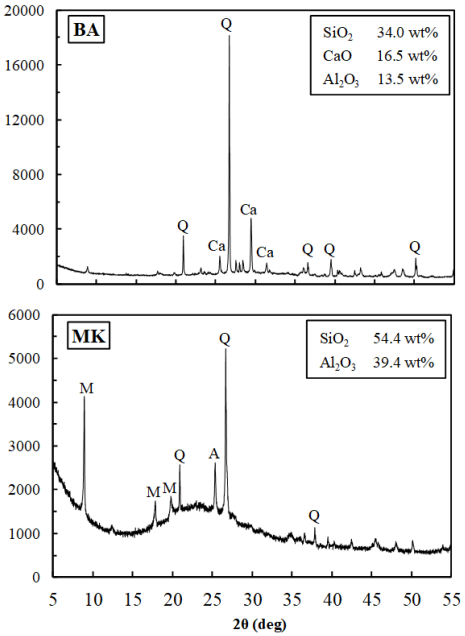

The particle size measured for BA was 32 μm (d_{50}), with spherical and asymmetric particles, as respectively observed in the particle size distribution and SEM micrograph in Figure 4.

Figure 4. SEM micrograph and particle size distribution of BA.

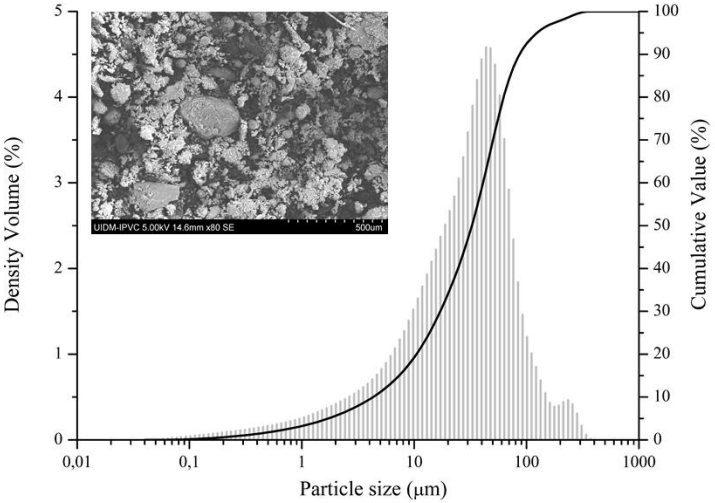

Thermogravimetric analysis of BA and MK is presented in Figure 5. For the BA ∽10 wt.% of total loss was detected, with ∽1.8 wt.% of loss being up until 250 °C, related with the endothermic residual moisture evaporation (Brown and Dykstra, 1995). Between 250 and 500 °C, there is a further mass loss (∽1.5%), whereas the DTA curve shows an exothermic peak (40 μV), typically associated with the organic material combustion, and finally from 500 to 800 °C, an endothermic reaction occurred due to $CaCO_3$ decomposition with ∽6% of mass loss (Simão et al., 2017). MK thermogravimetry, Figure 4, denoted lower total loss (~4 wt.%) when compared to BA, which can be expected from the metakaolin calcination process. However, a residual adsorbed and combined water (2.1 wt.%) evaporated endothermally up to 250 ºC. An exothermic peak at approximately 970 °C indicates mullite crystallization (Ramli and Alonge, 2016). The respective total mass loss values of BA (~10 wt.%) and MK (~4 wt.%) are comparable to those of ignition loss associated to XRF, considering the inherent uncertainty of both analyses.

Figure 5. Thermograms (TG - DTA) curves of biomass fly ash (BA) and metakaolin (MK).

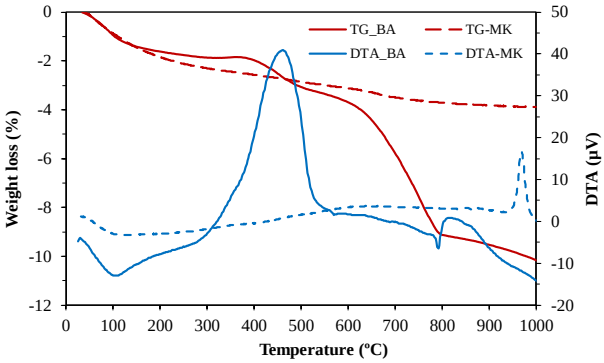

2.2.2. Effect of the alkaline activator's ratio on the geopolymers properties

Figure 6 shows that a higher sodium silicate to sodium hydroxide weight ratio (SS:SH = 1.5) caused an increase in mechanical strength when compared to SS:SH = 1.0, for all the curing methods studied. This strength gain is explained by the increase of the SiO_2/Al_2O_3 molar ratio (Table 1) resulting in formation of more Si–O–Si bonds, which are stronger than Si–O–Al and Al–O–Al bonds (De Jong and Brown, 1980; Leong et al., 2016). As evidenced in the study of CRIADO; PALOMO; FERNANDEZ JIMENEZ (2005), the addition of sodium silicate to the activating solution promotes the polymerization of the ionic species present in the system, and explains the development of high mechanical strength at higher SS:SH weight ratio (1.5). However, the mechanical strength results obtained for the geopolymers with SS:SH = 1.0 were still satisfactory, perhaps as a result of the high OH^- content maintained in this system throughout the activation process (Criado et al., 2005).

Figure 6. Compressive strength (CS) and bulk density (BD) of geopolymers developed with SS:SH = 1.0 and SS:SH = 1.5 (weight ratios) and different curing methods at 28 days.

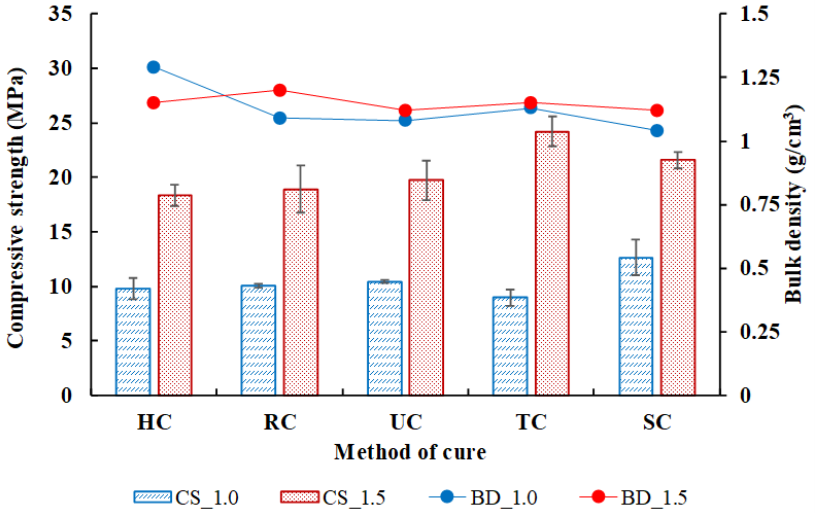

The bulk density results, Figure 6, showed low differences in the values with the different concentrations of alkaline activators. The increase in bulk density with the weight ratio SS:SH = 1.5 is associated to a higher amount of sodium silicate that increases the alkaline solution viscosity, contributing to the compactness of the network structures (Huseien et al., 2018). Geopolymers produced with SS:SH = 1.0 presented lower values of bulk density, with the exception of the geopolymer submitted to HC, which reached the highest value (1.29 g/cm³) of bulk density. This increase in bulk density is related to the densification process, where during the curing process the formation and the growth of zeolite crystals occurs, in hydrothermal conditions (Le et al., 2019).

Table 2 presents the water absorption of geopolymers with different curing methods and alkaline activators ratios. Regardless of the curing method used, with exception to HC, the samples produced with the lowest relative concentration of sodium silicate (SS:SH = 1.0) presented higher values of water absorption when compared to those produced with SS:SH = 1.5. This is explained by the increased amount of water available, generating higher porosity (lower density) and consequently higher water absorption.

Table 2. Water absorption of geopolymers produced with different curing methods and alkaline activators weight ratios (1.0 and 1.5) at 28 days.

Method	SS:SH = 1.0 (%)	SS:SH = 1.5 (%)
HC	29.32 ± 0.3	39.99 ± 0.3
RC	42.20 ± 1.1	35.59 ± 0.5
UC	43.34 ± 0.5	41.33 ± 0.5
TC	39.21 ± 0.6	38.21 ± 0.6
SC	47.74 ± 0.4	43.55 ± 0.1

The XRD spectra of geopolymers (cured for 28 days) are presented in Figure 7. The formation of a new amorphous material is observed between the angles of 25° and 35° (2θ), characterized by a hump and referred to as a geopolymer gel formation (De Rossi et al., 2019; Novais et al., 2016b; Provis et al., 2005). Quartz, calcite and muscovite peaks were also detected, corresponding to crystalline phases originating from the raw materials, BA and MK, with lower intensity. It seems that the mineralogical composition of the geopolymers was not affected by the different methods of cure tested. An exception was the sample HC-1.0, in which the development of new crystalline peaks was observed, through the conversion of geopolymer gel into crystalline zeolites (faujasite and zeolites P), as also detected in the literature for hydrothermal conditions, at the temperature range from 60 °C to 180 ºC (Lee et al., 2016; Liu et al., 2016b; Yan et al., 2012).

Figure 7. XRD patterns of geopolymers with different curing methods and weight ratios of SS:SH = 1.0 and 1.5 at 28 days, where Q = Quartz (PDF 00-046-1045); M = Muscovite (PDF 00-05-2035); Ca = Calcite (PDF 04-012-0489); P = Zeolite P (PDF 00-040-1464); F = Faujasite (PDF 04-014-0612).

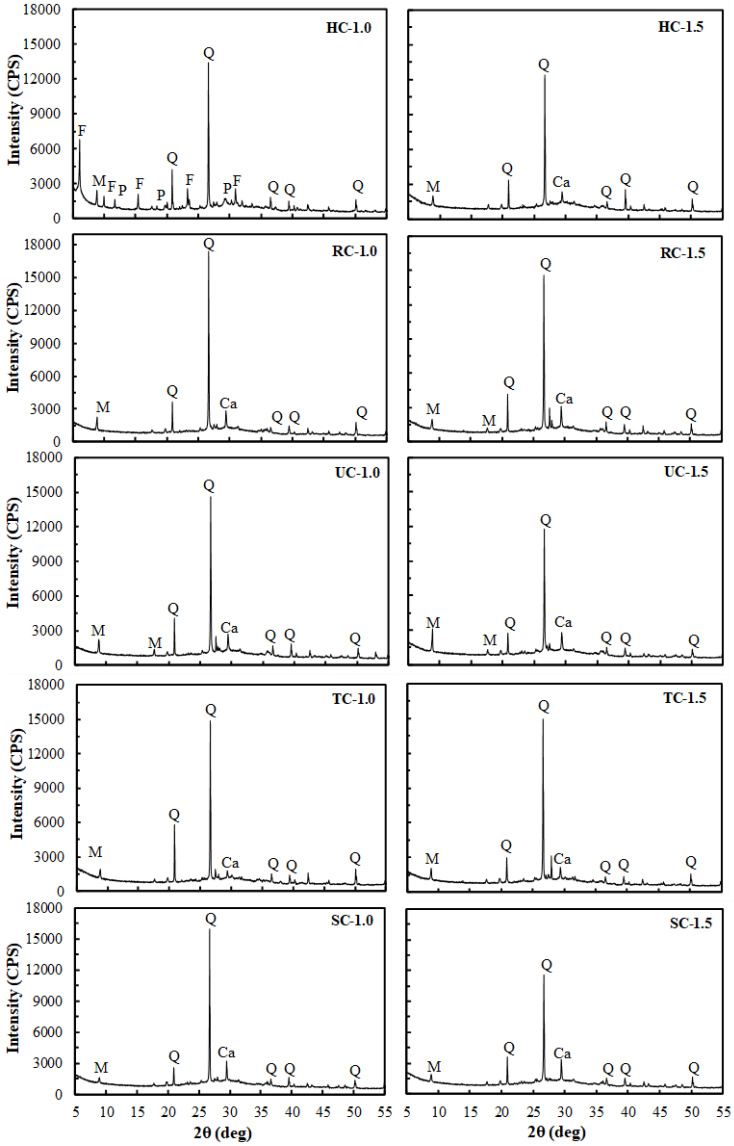

The formation of new crystals can be seen in a SEM micrograph (Figure 8). The presence of the crystalline zeolites might be related to the increased density (1.29 g/cm^3) and the lower value of water absorption (29%) for HC-1.0 (Mohseni, 2018; Mohseni et al., 2016).

Figure 8. SEM micrograph of HC-1.0 with new crystalline phases, where F = Faujasite and P = P zeolite.

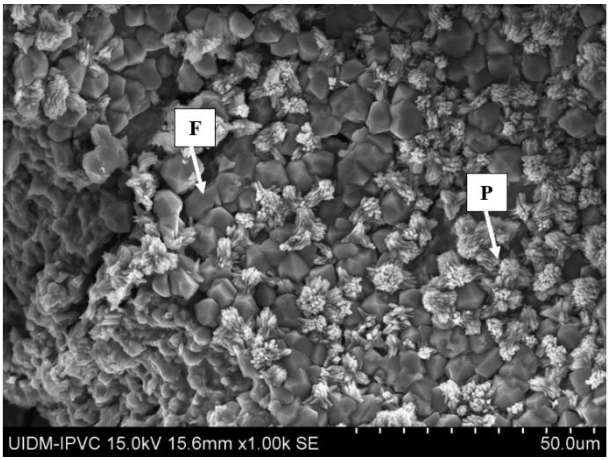

The XRD patterns show that the geopolymers developed with SS:SH = 1.5 presented less intense crystalline peaks when compared to those with SS:SH = 1.0, indicating the transformation of quartz and muscovite, BA and MK minerals, into amorphous geopolymerization products (Tuyan et al., 2018). Thus, the decrease in peak intensity confirms the increase in the dissolution of these oxides and the increase of the geopolymerization rate, contributing to the increase of the compressive strength.

SEM images and EDS spectrum of specimens produced with SS:SH = 1.0 and 1.5 and cured with HC, RC, UC, TC and SC are shown in Figure 9. It can be seen from the micrographs that geopolymers produced with SS:SH = 1.0 and 1.5 are microscopically similar in all curing methods. The EDS was used to perform a semi-quantitative analysis of the geopolymers and their respective reaction products. The formation of an aluminosilicate gel mainly composed of Si, Al and Na was observed in all compositions, which provides additional evidence of a geopolymerization reaction (Novais et al., 2016d; M. Zhang et al., 2014).

Figure 9. SEM micrograph and correspondingly EDS spectrum of geopolymers with five curing methods (TC, HC, RC, SC and UC) and SS:SH = 1.0 (a) and 1.5 (b) at 28 days.

a)

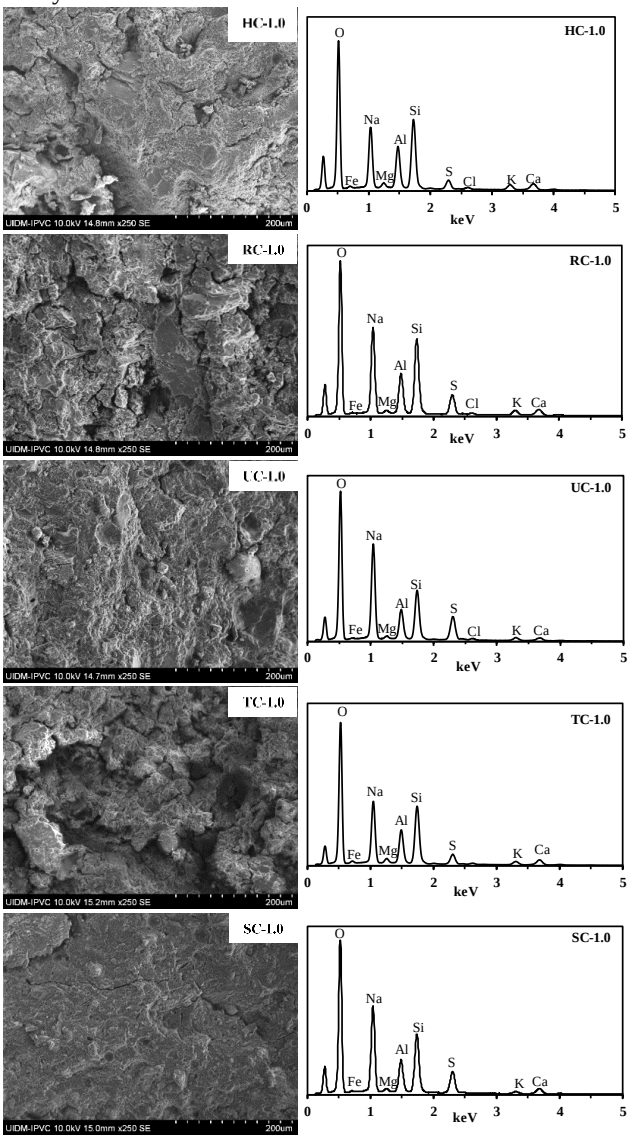

b)

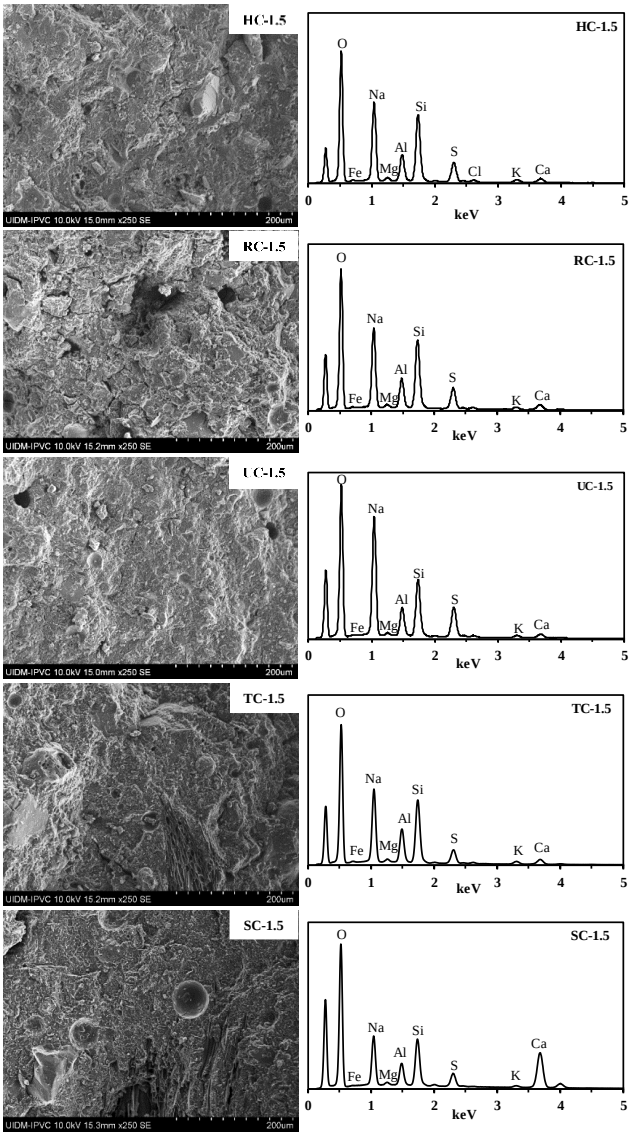

According to the thermogravimetric results, the total mass loss of the developed geopolymers with SS:SH = 1.0 ranged from 18.8% for TC to 45.6% for SC. For SS:SH = 1.5, and the mass loss was from 17.1% (TC) to 42.2% (SC). For the other cure methods, the values were within

this range as well. It is observed that the main differences of mass loss are associated with loss of free or interstitial absorbed water (Bagheri et al., 2018). The thermal events occurred were similar for all developed geopolymers and as discussed in the next section.

Figure 10. Thermograms (TG - DTA) curves of geopolymers submitted to five methods of cure (TC, HC, RC, SC and UC) with two alkaline activators weight ratios SS:SH=1.0 (-·-·-) and SS:SH=1.5 (·····).

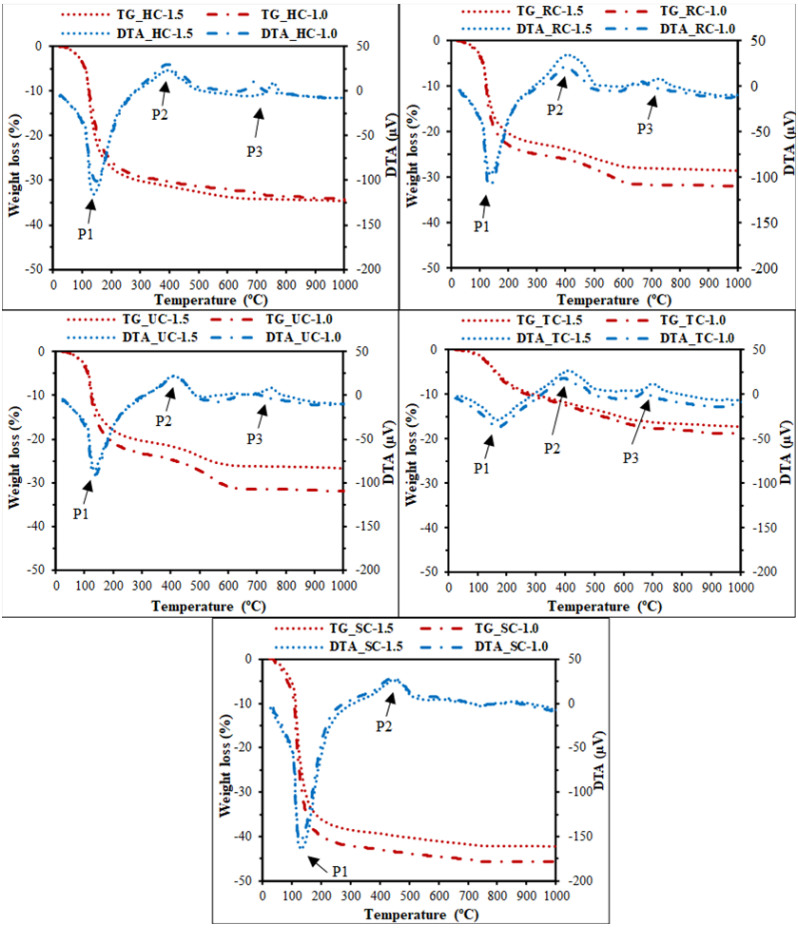

2.2.3. Discussion

For the curing methods HC, RC and UC, it was not possible to observe significant differences in the values of mechanical strength considering different weight ratios of SS:SH = 1.0 and 1.5. In the same way, bulk density does not have a greater difference between methods, staying within the standard deviations. Thus, the obtained results denote that the geopolymers process curing under environmental conditions of humidity and temperature (RC) may be the indicated method for the development of ecofriendly geopolymers (low economic and environmental costs) since equivalent mechanical properties or even superior are obtained when compared to the other methods tested.

The curing of geopolymers under hydrothermal conditions (HC) with SS:SH = 1.0 can be justified for the development of materials with specific characteristics, such as the production of zeolites (De Rossi et al., 2019; Khalid et al., 2018; Zheng et al., 2019), although at higher economic expenses and environmental impacts.

In our case, the UC method, which has been extensively used in studies to improve the geopolymers properties, did not increase the mechanical strength values and did not add any specific characteristics to the geopolymers. According to TURNER; COLLINS, (2013), curing at a temperature of 50 °C for 24 h increases the CO_2 emission in the geopolymer concrete production by 11%, thus showing that this curing method is not advantageous for the geopolymers development.

For thermal cure (TC), the use of SS:SH = 1.0 is not the most appropriate because it presents low mechanical strength. For TC-1.5, where the highest mechanical strength value of the compression was obtained, its use can be exploited to obtain pre-molded geopolymer materials with improved mechanical properties, although it adds an extra energy cost to maintain the cure temperature at 40 °C. As mentioned earlier, the energy consumed during the hardening process goes back to the issue of CO_2 emissions (Turner and Collins, 2013), which may not advisable.

The cured of geopolymers under submerged conditions (SC) is valid for sealing geo-sequestration or petroleum/oil wellbore (Giasuddin et al., 2013). Geopolymers can also be applied in environmental remediation, as pH regulators where high buffer capacity is required (Novais et al., 2016d), taking advantage of its high alkalinity. Curing geopolymers submerged in water may be an alternative for those with efflorescence problems, since excess sodium is leached during the process; thus, not affecting the final properties (Z. Zhang et al., 2014).

When analyzing the mechanical behavior with the different curing methods for SS:SH = 1.0, it was observed that the greatest variation (3.68 MPa) occurred from TC to SC. Thus, it was concluded that the water curing in SC, with humidity control, positively influenced the geopolymers mechanical strength, and when the temperature increases without moisture control, as in the case of TC method, the mechanical properties decreased. According to VAN JAARSVELD; VAN DEVENTER; LUKEY, (2002) geopolymers cured at higher temperatures for long periods can lead to the breakdown of their granular structure, resulting in the dehydration and excessive retraction by gel contraction during the cure process.

However, in geopolymers developed with SS:SH = 1.5, the highest mechanical strength was obtained for TC (24.21 MPa) and the lowest strength for HC (18.39 MPa). These two methods have the same curing temperature (40 °C), and the humidity control did not positively influence the mechanical strength, as in geopolymers with SS:SH = 1.0. Thus, it is believed that the increase of the SiO_2/Al_2O_3 molar ratio by the addition of sodium silicate did not affect the mechanical strength due to dehydration, since larger amounts of Si were available for reaction, accelerating the geopolymerization process. Similar results in other studies have shown that higher cure temperatures between 30 and 90 °C are beneficial, especially in the first hours, because they promote the reactive species dissolution, allowing the geopolymers production with higher compressive strength (Bakharev, 2005; Palomo et al., 1999). In other words, higher concentration of silicate might contribute to higher strength development due to higher silicates availability for the geopolymerization (Palomo et al., 1999), that accelerate the stages of dissolution, nucleation, oligomerization, and polymerization. Nevertheless, they are not affected by the loss of water during cure at 40 °C, without moisture control, as this study also evidenced.

From the thermal analysis results (TG - DTA) of geopolymer samples shown in Figure 10, it is seen that weight loss for all specimens increases gradually with temperature (Komnitsas et al., 2015). The endothermic peak up to 200 °C, identified for P1 in the DTA curves, was observed for all samples caused by the adsorbed water evaporation, which is a normal result for mineral materials (Jin et al., 2018; Nikolov et al., 2017). In this event mass loss was different for each curing method, due to the process conditions used and to the loss of water physically absorbed (Al Saadi et al., 2017; Badanoiu et al., 2015; Bai et al., 2019). The lowest mass loss was obtained with TC (7.6% in 1.0 and 7.1% in 1.5), where the water available on the surface of the sample was evaporated, during the

curing process without moisture control, thus reducing the humidity of the sample. The largest mass loss was observed with the SC geopolymer (39.8% in 1.0 and 36.2% in 1.5) where the surface and pores of the sample were saturated, because the samples were submerged in water.

Between 200 - 600 °C, the loss of mass is attributed to the elimination of water and hydroxyl structural groups, Si-OH and Al-OH (Alomayri et al., 2013; Bagheri et al., 2018; Duan et al., 2017; Jin et al., 2018). identified as P2. According to WEN et al., (2019) the exothermic peaks occurred in this case between 700 - 800 °C, and identified in Figure 9 as P3, represented a crystalline phase of transition.

2.3. REMARKS

The results of this study showed that curing methods and relative ratios of alkaline activators can affect the physical and chemical properties of geopolymers.

Increasing SiO_2/Al_2O_3 ratios causes a positive influence on geopolymers mechanical resistance to compression, as expected from the literature. Otherwise, when geopolymers are developed for other applications, such as pollutant adsorbents, a lower SS:SH relative concentration is preferred in order to achieve a suitable porosity.

When curing was carried out in environmental conditions, a similar mechanical strength was obtained when compared to the methods usually adopted in the literature, which need higher energy consumption. This result brings an important contribution, enhancing the economic and environmental benefits of geopolymers and favoring their application.

3. EFFECT OF THE PARTICLE SIZE RANGE OF CONSTRUCTION AND DEMOLITION WASTE ON THE FRESH AND HARDENED-STATE PROPERTIES OF FLY ASH-BASED GEOPOLYMER MORTARS[2]

In this chapter, the valorization of industrial wastes (biomass fly ash and construction and demolition waste (CDW)) through the production of geopolymer mortars was studied. The effect of the sand substitution by CDW and the influence of the particle size range of CDW fine aggregates on the fresh and hardened properties of the mortars were evaluated.

The European Commission has identified construction and demolition waste (CDW) as a priority stream for reuse, highlighting the environmental benefits of its recovery (Directive 2008/98/EC, 2008; Pacheco-Torgal et al., 2012). It is estimated that the construction industry generates about 860 million tons of waste per year in the European Union, representing 34% of all waste produced (Eutostat, 2014). In some European countries, such as Denmark, Germany, Ireland, Netherlands and Estonia, the CDW recycling rates reach over 80% (Villoria Saez et al., 2011). In developing countries, such as Brazil, only 21% of CDW is recycled (Miranda et al., 2016). CDW has been increasingly recycled as aggregate in the production of new construction products, including concrete (Raeis Samiei et al., 2015).

Alternatively, CDW has been used to produce geopolymers (Komnitsas et al., 2015; Zaharaki et al., 2016). These novel binders may present properties comparable to those of Portland cement, but with a much lower CO_2 footprint (Davidovits, 1994; Provis and Bernal, 2014). A rigid control of the particle size and chemical composition of silicates and aluminates sources is required to obtain the suitable characteristics. Usual raw materials employed in geopolymerization are fly ash, blast furnace slag, and metakaolin (calcined clay) (Khale and Chaudhary, 2007). Some studies have demonstrated that metakaolin could be completely/partially replaced by biomass fly ash (Novais et al., 2018b) or powdered CDW (Komnitsas et al., 2015; Vásquez et al., 2016; Zaharaki et al., 2016).

CDW can be also used as fine aggregates to produce mortars, which is a more attractive application, since the particle size required in

[2] Accepted for publication in *Process Safety and Environmental Protection*.
https://www.sciencedirect.com/science/article/pii/S0957582019304914

this case is coarser than that to corresponding to geopolymer binders. However, the mechanical properties of the mortars produced from CDW, such as flexural strength and compressive strength, decrease as the amount of recycled aggregates in the mortar increases (Silva et al., 2016).

Research targeting the use of CDW as aggregate in geopolymers is scarce (Cristelo et al., 2018; Mohammadinia et al., 2016). Nevertheless, fine sized CDW (d_{50} = 0,39 mm) was considered an adequate aggregate to be used in alkali activated fly ash, since no effect on the strength value during or after activation reactions was observed. CDW might act as filler but the finer fraction might even react with the activator (Cristelo et al., 2018), partially acting as binder in the geopolymerization process. Nevertheless, the influence of the particle size on the characteristics of geopolymer mortars was not fully evaluated, being this the main objective of the current work. We observed that is possible to produce geopolymer mortars with enhanced mechanical strength by adjusting the CDW particle size, used as alternative aggregate to natural sand.

3.1. EXPERIMENTAL

3.1.1. Fine Aggregates

The dense mortars were prepared using the standard mixture of BA and MK as binder, and CDW as fine aggregates. The CDW samples used in this work were sieved in two fractions: 0.5-1.0 mm, 1.0-2.0 mm; one third fraction (0.5-2.0 mm) was obtained by mixing (1:1 wt.%) the two sieved fractions. Normalized sand used as fine aggregate was commercially supplied (Mibal, Barqueiros, Portugal) with similar particles size distribution of the prepared CDW. CDW 0.5-1.0 mm and 1.0-2.0 mm fractions were visually selected in brick and concrete particles for characterization.

3.1.2. Mortar preparation and flow characterization

The geopolymer mortars were prepared using binder: aggregate weight ratio = 1:3, the mix design of samples prepared in this study was presented in the Table 3. The binder (BA and MK), aggregates (CDW or sand) and alkaline activators (SS and SH) were added to the mixer, following the steps: i) initial homogenization of sodium silicate and NaOH solution at 60 rpm for 5 min; ii) mixture at the same speed of the alkaline solution with solids materials for 10 min, and iii) homogenization and mixture for another 5 min at 95 rpm.

The mixture was maintained under agitation until the materials were completely impregnated. The alkaline solution was the only liquid component in all mixtures (no water addition).

The effect of the replacement of natural by recycled aggregate and of different particle sizes, 0.5-1.0 mm, 1.0-2.0 mm and 0.5-2.0 mm, on the rheological behavior of mortars was evaluated. Flow measurements of fresh mortars were performed according to ASTM C 1437 (2007) and the results were expressed as spread diameter.

Table 3. Mix design of geopolymer mortars with CDW and sand (wt.%).

Mortar	CDW	Sand
Binder	20	20
Alkaline activator	20	20
Aggregate	60	60

3.2. RESULTS AND DISCUSSION

Materials used as sources of aluminosilicates (BA and MK) and as fine aggregates (CDW and sand) have the chemical compositions shown in Table 4. As expected, in sand the dominant oxide was SiO_2, and in MK were SiO_2 and Al_2O_3. In the BA and CDW, the main components were SiO_2, Al_2O_3 and CaO. The composition of CDW is variable, as expected, but falls reasonably within the weight ranges referred in the literature: 40-70 wt.% SiO_2, 5-20 wt.% Al_2O_3, 10-25 wt.% CaO, and 0.5-8 wt.% Fe_2O_3 (Contreras et al., 2016; Saiz Martínez et al., 2016; Vásquez et al., 2016).

Table 4. Chemical composition (wt.%) of BA, MK, sand and different fractions of CDW.

Oxides		SiO_2	Al_2O_3	MgO	CaO	Na_2O	K_2O	Fe_2O_3	TiO_2	SO_3	LOI
	BA	34.00	13.50	3.10	16.50	1.50	5.50	5.00	0.60	2.80	14.30
	MK	54.40	39.40	0.14	0.10	-	1.03	1.75	1.55	-	2.66
	Sand	98.90	0.10	0.11	0.22	0.15	0.35	0.02	0.06	0.09	-
CDW	0.5-1.0 mm	70.51	8.01	1.11	9.62	0.16	1.80	2.27	0.32	0.41	5.48
	1.0-2.0 mm	69.48	8.67	1.19	8.73	0.16	1.84	2.54	0.34	0.38	6.44
	brick	58.53	19.73	2.44	3.29	0.28	4.16	6.45	0.78	0.11	3.87
	concrete 0.5-1.0 mm	75.40	0.64	0.64	10.37	0.13	0.99	0.93	0.17	0.46	6.48
	concrete 1.0-2.0 mm	69.51	0.75	0.75	15.41	0.14	0.99	1.07	0.20	0.71	6.35

LOI = Loss on Ignition.

The particle size distribution of CDW can be seen in Figure 11a. After milling, ∽65 wt.% of particles are between 0.5 - 2.0 mm. Figure 11b shows SEM and optical photographs of CDW particles. In the Figure 11b, it is possible to visually observe the CWD composition from the optical photos and SEM micrographs, consisting basically of concrete and clay brick particles in the size ranges of 0.5-1.0 and 1.0-2.0 mm.

Figure 11. Characteristics of CDW: a) Particle size distribution; b) SEM micrographs (left) and optical photos (right) of CDW samples: I) 0.5-1.0 mm and II) 1.0-2.0 mm.

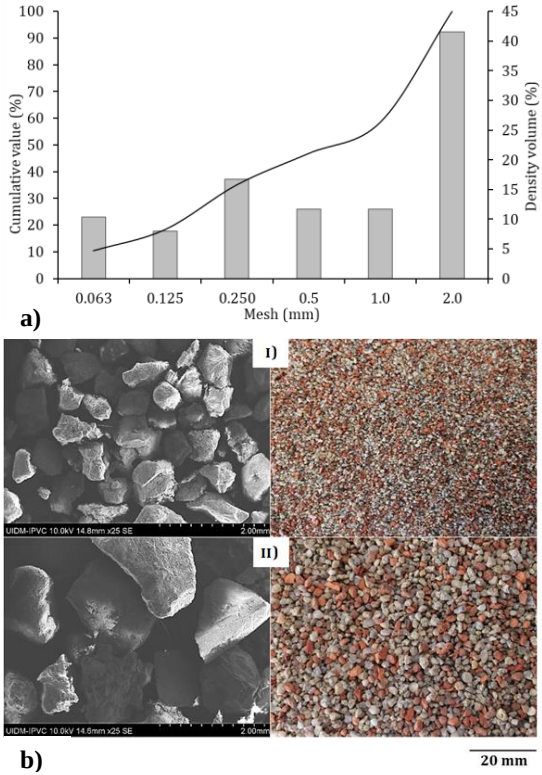

They also reveal the irregular shape of the grains, which causes ∽ 20% reduction in the bulk density of the recycled aggregates compared to sand (Table 5), this effect is related to the greater packing of the spherical particles of the sand.

Table 5. Physical properties of aggregates and geopolymer mortars.

Aggregate	Particle size (mm)	Aggregate density (g/cm^3)	Water absorption (%)	Bulk density (g/cm^3)	Porosity (%)
CDW	0.5 - 1.0	1.25 ± 0.04	12.1 ± 0.1	1.78 ± 0.02	21.5 ± 0.19
	1.0 - 2.0	1.21 ± 0.04	12.3 ± 0.2	1.83 ± 0.01	22.5 ± 0.29
	0.5 - 2.0	1.29 ± 0.07	12.3 ± 0.1	1.82 ± 0.01	22.3 ± 0.15
Sand	0.5 - 1.0	1.52 ± 0.05	11.7 ± 0.1	1.83 ± 0.01	21.5 ± 0.18
	1.0 - 2.0	1.46 ± 0.05	11.6 ± 0.2	1.91 ± 0.01	21.8 ± 0.20
	0.5 - 2.0	1.54 ± 0.06	12.2 ± 0.2	1.89 ± 0.01	22.7 ± 0.17

XRF results of CDW 0.5-1.0 and 1.0-2.0 mm fractions are similar, revealing that the grain size fractioning does not significantly alter the chemical composition. However, by segregating the brick and concrete fraction of the CDW, compositional changes were observed (Fig. 12).

Initially, in the 1.0-2.0 mm fraction, brick and concrete components correspond to 27 wt.% and 73 wt.%, respectively. In the 0.5-1.0 mm fraction, the brick amount decreased to 17.4 wt.%. This is expected, since the concrete is composed of finer elements (cement and sand) than bricks, being segregated upon grinding. This is confirmed by FRX results, revealing a ∽6% increase in the SiO_2 content in the concrete fraction in the particle size of 0.5-1.0 mm, as shown in Table 2.

Figure 12. Composition (wt.%) of bricks and concrete in the CDW aggregates of sizes 0.5-1.0 and 1.0-2.0 mm, respectively.

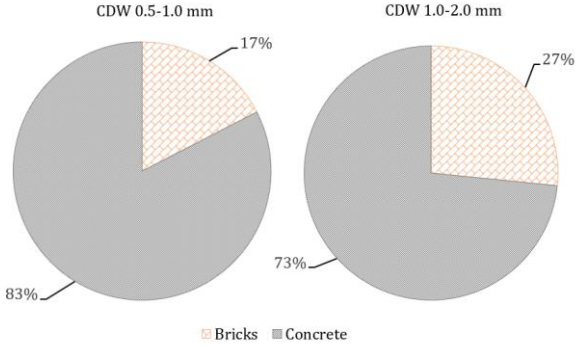

The mineralogical compositions of the raw materials used are given in Figure 13. The identified crystalline phases in CDW were quartz (PDF 00 046 1045), calcite (PDF 04 012 0489) and muscovite (PDF 00 058 2035). In the XRD patterns of BA were identified quartz and calcite, and quartz and muscovite in the MK, as presented in previous work (De Rossi et al., 2018). Similar composition was found elsewhere for fly ash (Arenas et al., 2017; Mehta and Siddique, 2017) and CDW (Arenas et al., 2017; Contreras et al., 2016; Vásquez et al., 2016).

Figure 13. XRD patterns of raw materials (CDW and BA) and the geopolymer mortars with CDW 0.5-2.0 mm and sand 0.5-2.0 mm. Q = Quartz (PDF-00-046-1045); M = Muscovite (PDF-00-05-2035); C = Calcite (PDF-04-012-0489).

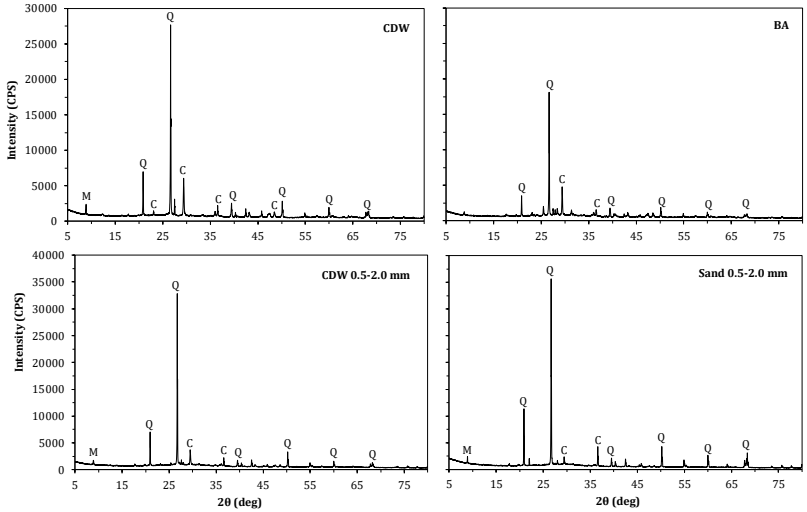

The fly ash presents an halo visible approximately 2θ between 17° and 33°, revealing its amorphous or vitreous character (Cristelo et al., 2018). In this fly ash, no halo was identified, evidencing low potential for geopolymerization. However, it is supposed that if formulated correctly with MK, it could be used as a binder for geopolymers, as demonstrated by NOVAIS et al., (2016b) and (De Rossi et al., 2019). The mortars produced with CDW and sand with particle size of 0.5-2.0 mm present the same minerals of the raw materials, as can be also observed.

3.2.1. Flow measurements of fresh geopolymer mortars

The results of the flow table test presented in Fig. 14 show that the mortars developed with CDW had smaller scattering diameters, when replacing the natural aggregate (sand), in all size ranges. This behavior is related with the lower sphericity of the CDW particles (Moreno, 2005), enhancing the internal attrition/friction between particles (Senff et al., 2009), reduced the flowability of mortars.

Figure 14. Flow diameter of geopolymer mortars with CDW and sand aggregates.

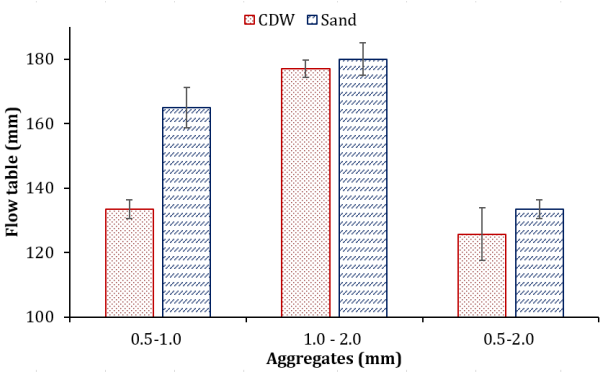

The lowest spread values were registered on mortars prepared with aggregates of broader size distribution (0.5-2.0 mm): 126 mm and 133 mm, respectively for CDW and sand. The extended particle size range will increase the packing density of the fresh mortars, and more compact systems shown higher yield stress values. Similar results were found in the literature using fine CDW aggregates for cement mortars (Fan et al., 2015; Topçu and Bilir, 2010; Torkittikul and Chaipanich, 2010).

3.2.2. Physical properties and mechanical behavior of hardened geopolymer mortars

The properties of hardened mortars samples are listed in Table 5. The water absorption results were similar for all mortars produced (∽12%), which is in accordance with the results obtained by MERMERDAŞ et al., (2017a), using natural sand as an aggregate for geopolymer mortars. Nonetheless, CDW and sand mortars have a similar porosity (∽22%) after 28 days of curing period, showing the viability of CDW reuse as fine aggregate. The results of the mortars bulk density show that the natural aggregate replacement by the recycled aggregate, in all size ranges, influences the obtained results. Thus, the mortars produced with CDW presented a lower density compared to the sand mortars, which are in agreement with several works showing that, by increasing the amount of recycled aggregate, the density of mortars decreases (Hwang et al., 2008; Silva et al., 2016).

In the thermal conductivity tests (Figure 15a), mortars produced with CDW aggregate presented values between 0.70 and 0.81 W/m·K,

lower than those obtained when using sand as aggregate (0.87 and 0.91 W/m·K).

Figure 15. Physical properties of hardened geopolymer mortars: a) Thermal conductivity; b) Compressive strength; c) Flexural strength.

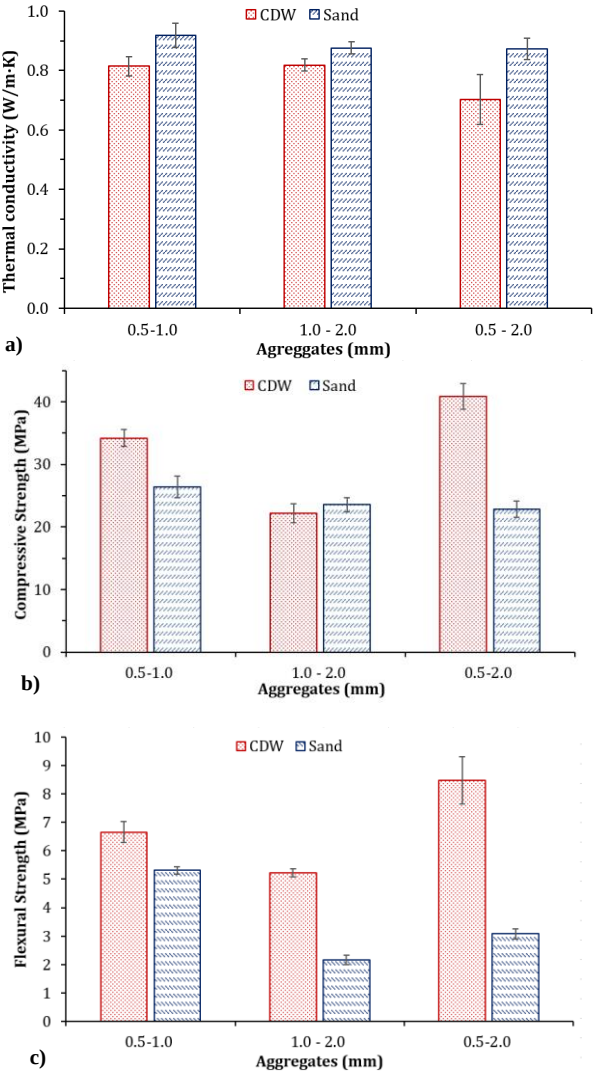

These results are related to the density of the studied aggregates, higher aggregates' density increases solid conduction and consequently thermal conductivity increases (Gomes et al., 2017) of mortar with sand. For CDW mortars, the lower density of the residues associated with the porosity of the residues influenced the lower values of thermal conductivity, as shown in Table 5. Similar thermal conductivity results were obtained by NARAYANAN; SHANMUGASUNDARAM, (2017), when investigating geopolymer mortars with natural sand, 0.91 W/m·K.

The compressive strength values for geopolymer mortars with CDW and sand are shown in Figure 15b. The highest strength was achieved when CDW was used as aggregate, except for the mortar produced with the particles of 1.0-2.0 mm, when higher resistance was obtained with sand. The obtained results for CDW-geopolymer mortars were ∽21 MPa (1.0-2.0 mm), ∽34 MPa (0.5-1.0 mm) and ∽40 MPa (0.5-2.0 mm). The highest strength values were obtained for the mixed fraction, due to the highest packing density (Reig et al., 2017; Sohn and Moreland, 1968).

Considering EN 998-2, (2010) standard, they can be classified as M20 (>20 MPa) and Md (>25MPa), for masonry mortars have compressive strength, after 28 days. However, it is important to note that there are still no standards for the mortars produced by geopolymerization (only for geopolymer concrete standard PAS 8820, (2016) so that the use of the standard EN 998-2, (2010) was only for comparison with commercial cement-based mortars.

Figure 15c presents the flexural strength results of the mortars cured during 28 days at room conditions. When comparing to sand used as aggregate, the best performance was obtained again with the mortars produced with CDW as aggregate. When the extended range of particles was used (0.5-2.0 mm), the highest values of flexural strength were obtained (8.5 ± 0.8 MPa), following the tendency of the compression strength results. Thus, the larger distribution of aggregate sizes increases the packing density of mortars, as observed elsewhere (Contreras et al., 2016; Mermerdaş et al., 2017b; Reig et al., 2017; Sohn and Moreland, 1968).

Similar results were also obtained in other studies, where it is suggested that the cement mortars produced with CDW fine fractions developed higher mechanical resistance, when compared with natural aggregates (Neno et al., 2014; Topçu and Bilir, 2010). This increase in the mechanical strength may be associated with chemical reactions of the non-hydrated cement particles present in CDW (Braga et al., 2014) or to the pozzolanic reactions between alumina, silica and calcium hydroxide

available in cement (Vieira et al., 2016) and also because the concrete particles have a higher specific surface and more porous than sand, promoting the better bond with the cement paste (Neno et al., 2014). Thus, other factors that generally affect the mechanical properties of mortars, such as porosity and water absorption, did not influence the results obtained in this study.

Photos of CDW and sand hardened mortars samples are compared in Figure 16. It is possible to observe that the aggregates used, CDW and sand, were totally integrated into the geopolymer paste, forming a homogeneous and compacted microstructure. Thus, no preferential paths are visible, which facilitate the rupture of the hardened mortar. The content of brick particles in the CDW aggregate and the presence of some porosity can be also observed in all samples. The residual porosity is probably due to the absence of vibration in the fresh mortar, but it did not compromise the good performance in the mechanical behavior as seen previously.

Figure 16. Photos of geopolymer mortar samples with CDW (a, b, c) and sand (d, e, f) as fine aggregates.

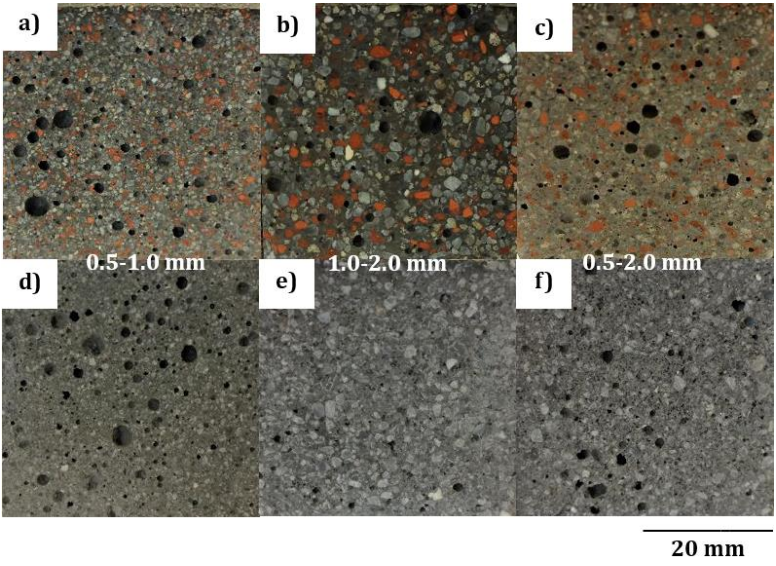

In Fig. 17 presented the semiquantitative chemical composition by EDS of geopolymer mortars with recycled and natural aggregate, for a particle size of 0.5-2.0 mm. It is observed that the chemical elements

identified were Si, Al, Na, K and Ca in both mortars analyzed. It was detected that in the mortar produced with sand, an increase in the silicon peak is observed, due the sand presence (with 98 wt.% of SiO_2).

Figure 17. SEM micrographs and EDS spectra of mortar paste with a) CDW 0.5-2.0 mm and b) sand 0.5-2.0 mm.

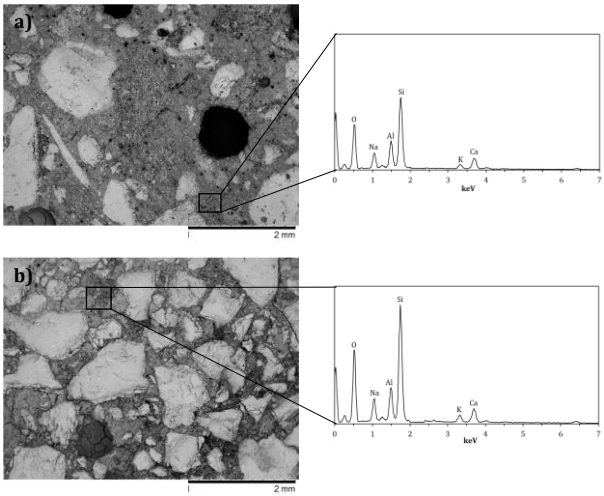

The lower results obtained with the mortar developed with natural aggregate can be attested by SEM micrographs (Fig. 17b). Here microcracks are observed in the interface region of the natural aggregate and the geopolymer paste, which induce the easily rupture of the specimens and reduce the compressive and flexural strength of hardened mortars. These microcracks were not observed in the microstructure of mortars produced with CDW, thus reiterating the advantages of the recycled fine aggregate using in the production of geopolymer mortars.

3.3. REMARKS

In this work, the geopolymer mortars produced with biomass fly ash as a binder and CDW as fine aggregate and cured in environmental conditions exhibited enhanced mechanical and flexural strength, exhibited increase 78% in mechanical strength and 175% flexural strength, in comparison with the sand as fine aggregate (0.5-2.0 mm).

In the fresh state, mortars produced with CDW showed less dispersion compared to the sand aggregate samples, possibly due to the

higher absorption of water by this industrial waste. However, in the hardened state, the highest mechanical strength results were obtained with CDW with a wide range of particles (0.5-2.0 mm), due to the higher packaging of the particles and microcracks absence. The results obtained for porosity, density and water absorption show total compatibility between mortars produced with CDW in substitution of sand as aggregate. Thus, the possibility of adding CDW as a fine aggregate in the production of geopolymer mortars has been proven, with excellent mechanical properties and potential for several applications in building, replacing conventional mortars.

In addition, 75 wt.% of the materials used in the production of geopolymer mortar are industrial wastes (BA and CDW). The use of wastes as raw materials reduces the exploitation of natural resources and highlights the environmental and economic advantages of recycling.

4. WASTE-BASED GEOPOLYMER MORTARS WITH VERY HIGH MOISTURE BUFFERING CAPACITY[3]

In this chapter, for the first time, lightweight waste-based geopolymer mortars were evaluated regarding their potential to passively adjust indoor relative humidity (RH) levels. Geopolymer mortars were prepared using a mixture of fly ash (BA) and metakaolin (MK) as a binder, in a proportion of 75:25 wt.% (BA:MK), construction and demolition waste as the fine aggregate and a pore forming agent in varying amounts.

The development of novel building materials with improved moisture buffering capacity is growing due to the energy consumption associated with mechanical heating, ventilation and air-conditioning (HVAC) systems in buildings (Zhang et al., 2017). Besides the economic aspects, high indoor humidity levels can cause condensation on interior surfaces, material defacement and the proliferation of microorganisms with negative effects on human comfort and health (Di Giuseppe and D'Orazio, 2014; Zhang et al., 2017). Thus, the use of alternative materials, devices and approaches to minimize the use of HVAC systems and consequently to reduce the energy demand in buildings has been recently proposed. A promising alternative is the use of novel materials to control the indoor hygrothermal conditions passively (Gianangeli et al., 2017).

The mechanism of moisture diffusion in hygroscopic materials is dependent on the moisture capacity and water vapor or liquid permeability. The moisture buffer value (MBV) is used as an unequivocal measure to characterize this property of building materials. This is a direct measurement of the amount of water vapor adsorbed or desorbed by a hygroscopic material when it is exposed to a periodic wave in daily cycles (Rode et al., 2007). A hypothetical example of such cycles could be 12 h of higher relative humidity (RH = 75%) followed by 12 h of lower relative humidity (RH = 50%). It has being reported that the energy saving increases with increasing MBV values (Zhang et al., 2017).

Different studies have shown that materials commonly used in building and construction (wood and wood-based components (Hameury, 2005; Hameury and Lundström, 2004; Osanyintola et al., 2006), modified mortars (Gonçalves et al., 2014b, 2014a; Senff et al., 2015), and cellulose insulation (Padfield, 1999) or furnishings (textiles, wood and paper)

[3] Published in *Construction and Building Materials* 191 (2018) 39-46. https://doi.org/10.1016/j.conbuildmat.2018.09.201.

(Svennberg K, Hedegaard L, 2004), can be used for indoor moisture buffering. Modified mortars with enhanced moisture buffering can be produced using a porogenic additive (aluminum powder, sodium olefin sulfonate or superabsorbent polymers) (Gonçalves et al., 2014b, 2014a; Senff et al., 2016, 2015) or an aggregate (sand, zeolite, perlite, biomass waste) (Giosuè et al., 2016; Tittarelli et al., 2015). Although the MBV of these modified mortars is improved, all of these materials are classified as "moderate" ($0.5 < MBV < 1.0$) or "good" ($1.0 < MBV < 2.0$) (Rode et al., 2007) in terms of their moisture buffering capacity. Moreover, these mortars contain Portland cement, which has excellent binder properties but its use is considered unsustainable due to the high level of CO_2 emissions arising from its production (Chen et al., 2010). One eco-friendly alternative to Portland cement is the use of geopolymers. Geopolymers are synthesized by mixing solid aluminosilicates with alkaline activators at low temperatures (below 100 ºC) (Novais et al., 2018b, 2016d). This exciting technology also allows the use of various waste streams as raw materials (Novais et al., 2017, 2016b) which further decreases the production cost and carbon footprint. However, despite the promising properties of these innovative binder systems the possibility of using geopolymer mortars as moisture buffer materials remains unexplored.

In this study, lightweight waste-based geopolymer mortars were prepared using varying amounts of hydrogen peroxide (pore-forming agent) to produce very high moisture buffering eco-friendly materials, able to provide an efficient control of indoor humidity levels.

4.1. EXPERIMENTAL

Mortars were produced using the standard mixture of BA and MK, and the construction and demolition wastes (CDW) were used as the fine aggregate, fraction of 0.5-1.0 mm, and the binder: aggregate ratio was 1:1 (by weight). The grain size distribution curve of the fine aggregate is given in Figure 18.

Figure 18. Size distribution curve of the fine aggregate of CDW.

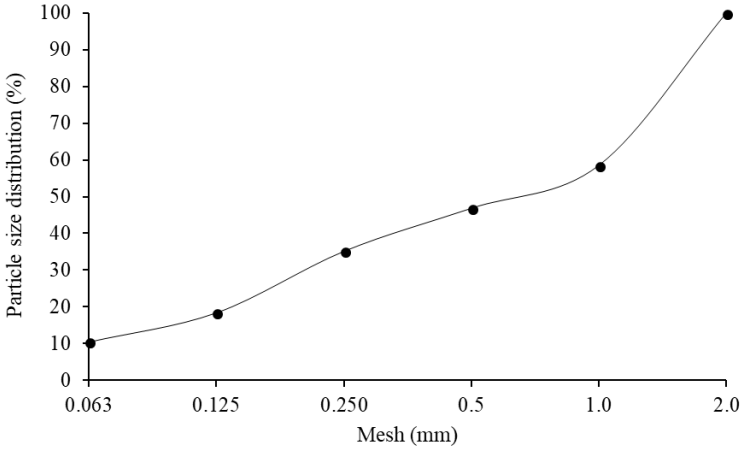

4.1.1. Geopolymer mortar preparation

The alkaline activators were previously mixed by agitation at 60 rpm for 5 min, and all solid materials (BA, MK and CDW) were added to the reactor. The mixture was maintained under agitation (60 rpm) for 10 min until complete homogenization was achieved. The H_2O_2 was then added in the appropriate amount and the mixture was homogenized for 2 min at 95 rpm (Novais et al., 2016a). In the next step, the geopolymer mortars were transferred to prismatic molds (40 mm x 40 mm x 160 mm), cylindrical molds (22 mm x 44 mm) and circular molds (12 mm x 94 mm) for the thermal conductivity, compressive strength and MBV measurements, respectively (Rode et al., 2007). The samples were removed from the molds after 24 h and subsequently cured at ambient temperature (~20 °C) and humidity (~68%) for 28 days. Table 6 summarizes the composition of the samples prepared in this study.

Table 6. Mix design of geopolymer mortars (wt.%).

H_2O_2	BA	MK	CDW	Na_2SiO_3:NaOH
0.00	25.05	8.35	33.3	33.3
0.15	25.01	8.34	33.25	33.25
0.30	24.98	8.32	33.2	33.2
0.45	24.94	8.31	33.15	33.15

4.1.2. Moisture buffering tests

The MBV was determined through the Nordtest method [4], using a climate chamber (Fitoclima 300 EDTU Aralab). The mass variation of cylindrical samples (diameter = 90 mm and height = 10 mm) was continuously determined and the data was recorded during the cyclic variation of the moisture according to ISO 24353 (2008) at a constant temperature of 23 ºC.

The MBV was calculated through equation (1):

$$MBV = \frac{\Delta m}{(A \; x \; \Delta\%RH)} \qquad (1)$$

Where Δm is the mass variation, A is the exposed surface of the sample, and Δ%RH is the amplitude of the humidity variation. In this study, the specimens were first preconditioned at 63% relative humidity for 24 h and then the humidity levels inside the chamber fluctuated between 75% (12 h) and 50% (12 h), this corresponding to middle humidity levels according to ISO 24353 (2008). The humidity changes were imposed four times in order to obtain four adsorption/desorption cycles.

4.2. RESULTS AND DISCUSSION

4.2.1. Evaluation of moisture buffering performance

The mass evolution of the mortars during the cyclic variation of the ambient moisture is shown in Fig. 19. All specimens show a slight increase in mass after each adsorption/desorption cycle. Nevertheless, the weight gain is moderate and the rate of increase tends to decrease with the number of cycles. For the mortar with the highest porosity (containing 0.45 wt.% H_2O_2), the specimen mass increase was 0.8 wt.% after the 1st cycle and decreased to 0.2 wt.% after the 4th cycle. This result indicates that these samples do not have a strong tendency toward saturation.

Figure 19. Mass evolution of mortars with different hydrogen peroxide contents registered during cyclic variation of the ambient moisture: a) 0.00 wt.%, b) 0.15 wt.%, c) 0.30 wt.% and d) 0.45 wt.%.

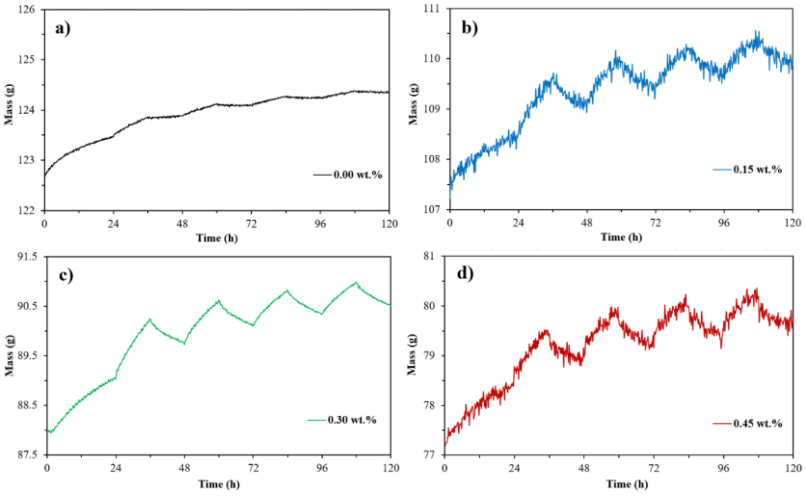

The mass evolution for the least porous mortar (prepared without H_2O_2) indicates a poor moisture buffer ability. In fact, the moisture adsorption and desorption rates for this mortar, shown in Fig. 20, confirm that the specimen was not efficient in terms of promoting indoor humidity control. The compositions containing different amounts of the pore-forming agent displayed distinct behaviors, as clearly demonstrated by the adsorption/desorption curves (see Fig. 19). Thus, the additional porosity promoted by the oxygen release, due to the H_2O_2 decomposition in the alkaline medium, plays a vital role in the moisture buffer ability of the mortars, with the MBV increasing from 0.80 g/m²Δ% RH (reference mortar) to 5.61 g/m²Δ%RH (higher porosity mortar). Nevertheless, the results show that desorption is less efficient that adsorption, that is, the moisture removal/desorption during exposure at 50% RH (12 h) does not fully compensate the adsorption that occurred in the previous step at 75 %RH (12 h). This result is in line with other studies performed with Portland cement mortars (Gonçalves et al., 2014a). The difference between the adsorption and desorption values shows that the geopolymer mortars studied have a low saturation tendency over time in an environment with humidity and temperature conditions similar to those applied in this study.

Figure 20. Moisture buffer value obtained from adsorption and desorption tests for the porous geopolymer mortars (cured for 28 days) with different amounts of porogenic agent.

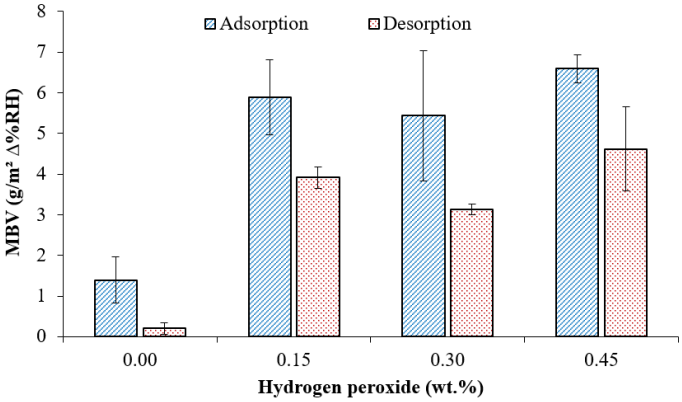

The highest MBV value (5.61 g/m²Δ%RH), obtained in this study for the mortar with the highest porosity, demonstrates the good potential of this waste-based material for promoting indoor moisture control. In fact, based on this result, according to the Nordtest classification method, this mortar shows excellent performance in terms of its moisture buffering capacity (> 2.0 g/m² Δ%RH) (Rode et al., 2007). Nevertheless, it should be highlighted that the humidity fluctuations imposed (following ISO 24353, 2008) differ from those prescribed in the Nordtest method (16 h at 33 %RH and 8 h at 75 %RH) and the final MBV value may differ slightly when using the Nordtest humidity fluctuations. This issue will be addressed in future work.

The maximum MBV observed for the BA-based geopolymer mortars was compared with previously reported values, as shown in Table 7. It can be observed that the results for the BA-based geopolymer mortars surpass all of the MBVs obtained in other studies, being 8 times higher compared with hydraulic lime mortars (Giosuè et al., 2016), between 2 and 5 times higher compared with cement mortars (Gonçalves et al., 2014b, 2014a; Senff et al., 2016, 2015) and around 3 times higher compared with lime-based plaster (Senff et al., 2017). The humidity fluctuations used here are similar to those used in (Senff et al., 2016) for cement mortar. In this study the authors reported an MBV of 1.3 g/m²Δ%RH, which is 4.3 lower than the one here reported. These results demonstrate the excellent moisture buffering capacity of the BA-based geopolymer mortars produced. To understand the phenomena involved in

the moisture adsorption by the porous geopolymer mortars, the analysis of adsorption-desorption moisture isotherms is fundamental and this will be discussed below.

Table 7 . Moisture buffer value (MBV) for mortars with different additives.

Materials	Porogenic agent	MBV (g/m²Δ%RH)	Cycles Temperature and Humidity	Reference
Cement mortar	superabsorbent polymer, vermiculite and perlite	∽ 2.5	5 cycles 75% (8 h) and 33% (16 h)	(Gonçalves et al., 2014b)
Cement mortar	aluminum powder, sodium olefin-sulfonate and superabsorbent polymer	1.3	5 cycles 75% (8 h) and 33% (16 h)	(Gonçalves et al., 2014a)
Cement mortar	superabsorbent polymer	∽1.1	5 cycles 75% (8 h) and 33% (16 h)	(Senff et al., 2015)
Cement mortar	superabsorbent polymer, vermiculite and TiO_2 nanoparticles	∽1.3	5 cycles 75% (12 h) and 53% (12 h)	(Senff et al., 2016)
Hydraulic lime mortar	spruce sawdust shavings, biomass bottom ash and biomass fly ash	0.7	5 cycles 75% (8 h) and 33% (16 h)	(Giosuè et al., 2016)
Lime-based plaster	cellulose fibers	1.9	5 cycles 75% (8 h) and 33% (16 h)	(Senff et al., 2017)
BA-based geopolymer mortar	H_2O_2 (0.45 wt.%)	5.6	5 cycles 75% (12 h) and 50% (12 h)	This study

4.2.2. Effect of porogenic agent concentration on phase composition and physical properties

The raw materials used to produce the geopolymer mortars present mainly SiO_2, Al_2O_3 and CaO in their chemical composition, as shown in Table 8. Quartz, calcite and muscovite were identified in the BA and CDW, while quartz and muscovite are the main minerals present in the MK (see Fig. 21). The mineralogical composition of the geopolymer mortars (GMs) produced showed the phases identified in the raw materials. The presence of H_2O_2 did not modify the mineralogical compositions of the geopolymer mortars (for the sake of brevity only one mortar composition is shown in Fig. 21), which is in agreement with findings reported by NOVAIS et al., (2016d).

Table 8. Chemical composition (in wt.%) of metakaolin (MK), fly ash (BA) and construction and demolition waste (CDW) determined by XRF.

Oxides	MK	BA	CDW
SiO_2	54.40	34.00	70.51
Al_2O_3	39.40	13.50	8.01
MgO	0.14	3.10	1.11
CaO	0.10	16.50	9.62
Na_2O	-	1.50	0.16
K_2O	1.03	5.50	1.80
Fe_2O_3	1.75	5.00	2.27
TiO_2	1.55	0.60	0.32
SO_3	-	2.80	0.41
LOI	2.66	14.30	5.48

Figure 21. XRD patterns for metakaolin (MK), fly ash (BA), construction and demolition waste (CDW) and geopolymer mortar containing 0.30 wt.% H_2O_2 (GM).

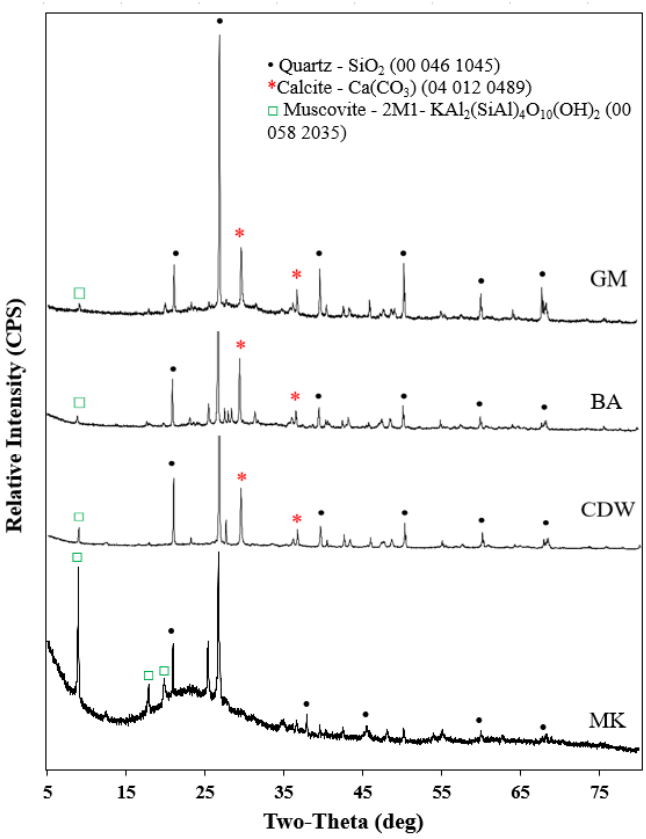

Table 9 shows the compressive strength, porosity, BET surface area and pore size for the different GMs. As expected, increasing the amount of H_2O_2 in the composition induces a decrease in the compressive strength of the specimen from 11.9 MPa to values ranging from 2.7 to 3.6 MPa, for compositions containing 0.30 and 0.45 wt.% H_2O_2, respectively.

Table 9. Mechanical, porosity and surface characterization of the porous geopolymer mortars.

H_2O_2 (wt.%)	Compressive strength (MPa)	Porosity (%)	BET surface area (m^2/g)	Pore size (μm)
0.00	11.9 ± 0.7	44.40	18.93	0.198
0.15	5.9 ± 0.8	47.79	24.40	0.786
0.30	2.7 ± 0.1	54.52	23.97	22.84
0.45	3.6 ± 0.2	55.92	26.70	31.88

The mortars solid to liquid ratio was intentionally kept at low levels in order to produce lightweight geopolymers. This is the reason why the reference mortar presents such high total porosity, despite the fact that no pore forming agent was been added to this composition. Thus, the reference mortar had exhibiting total porosity of around 44.40%, and the mortar with 0.45 wt.% H_2O_2 obtained 55.92%. Else, the compressive strength of mortar with 0.30% H_2O_2 is slightly lower than that with 0.45% of H_2O_2 even if the total porosity is almost the same. Further studies about the microstructure of these mortars using microtomography, for example, could explain these results.

Figure 22. Influence of the hydrogen peroxide content on the microstructure of geopolymer mortars: a) 0.00 wt.%, b) 0.15 wt.%, c) 0.30 wt.% and d) 0.45 wt.%.

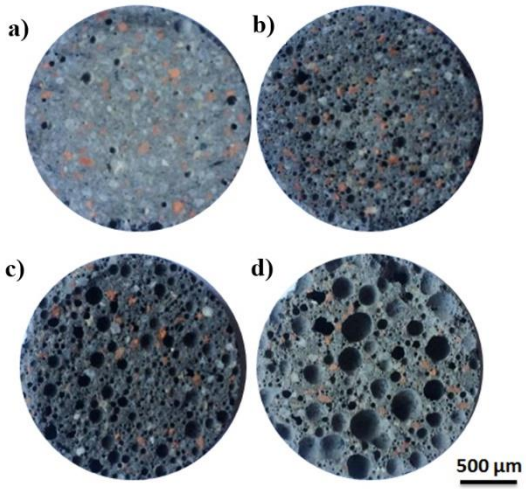

The results for the optical and SEM characterization of the GMs can be observed in Figs. 22 and 23. The micrographs clearly show an increase in the size and volume of the pores with increasing H_2O_2 concentration in the GMs.

Figure 23. SEM characterization of the geopolymer mortars prepared with different hydrogen peroxide contents: a) 0.00 wt.%, b) 0.15 wt.%, c) 0.30 wt.% and d) 0.45 wt.%.

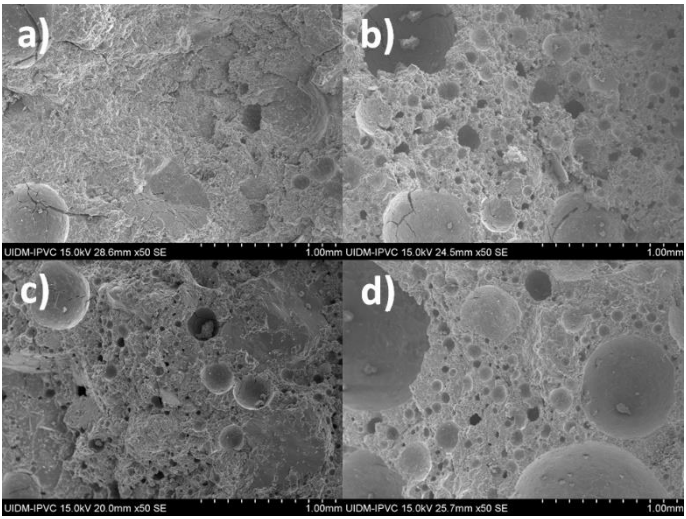

The N_2 adsorption and desorption isotherms (measured at 77 K) for the distinct mortars and the pore size distribution of the specimens, are shown in Fig. 24. While the results for the BET specific surface area (SSA) and pore size are reported in Table 4.

The GMs exhibited type II isotherms, which are characteristic of non-porous or macroporous solids (Brunauer et al., 1940). The pore size (Table 9) obtained from the mercury intrusion porosimetry were different for GMs, and macroporosity was prevalent, as seen by the inserts of Fig. 24. The SSA increased as the H_2O_2 concentration in the compositions increased, similarly to the pore size (Table 9) except in mortar with 0.30 wt.%.

Figure 24. Nitrogen adsorption (green diamonds) and desorption (red squares) isotherms and pore size distribution of the geopolymer mortars prepared with increasing hydrogen peroxide content: a) 0.00 wt.%, b) 0.15 wt.%, c) 0.30 wt.% and d) 0.45 wt.%.

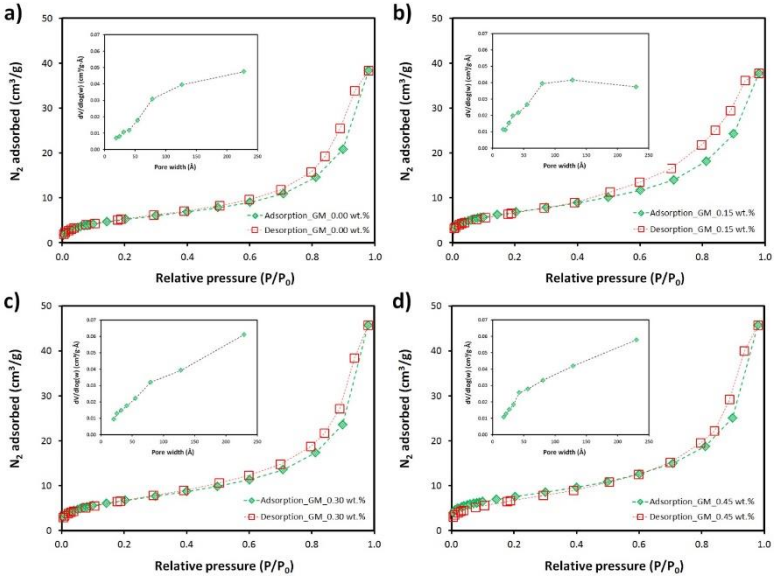

The results of the water absorption by capillarity tests performed on the porous mortars are shown in Figure 25. It can be observed that the addition of 0.15 and 0.30 wt.% H_2O_2 decreases the capillary index when compared to the reference mortar. This is because the addition of H_2O_2 leads to an increase in the quantity and size of the pores, affecting the capillary absorption by reducing the capillary pores. Moreover, although the GMs with 0.30 and 0.45 wt.% H_2O_2 presented similar total porosity, the pore size is different (Table 9), the addition of 0.45 wt.% H_2O_2 is expected to lead to a higher amount of interconnected pores than 0.30 wt.% H_2O_2.

Figure 25. Capillary water absorption of mortars prepared with different hydrogen peroxide contents.

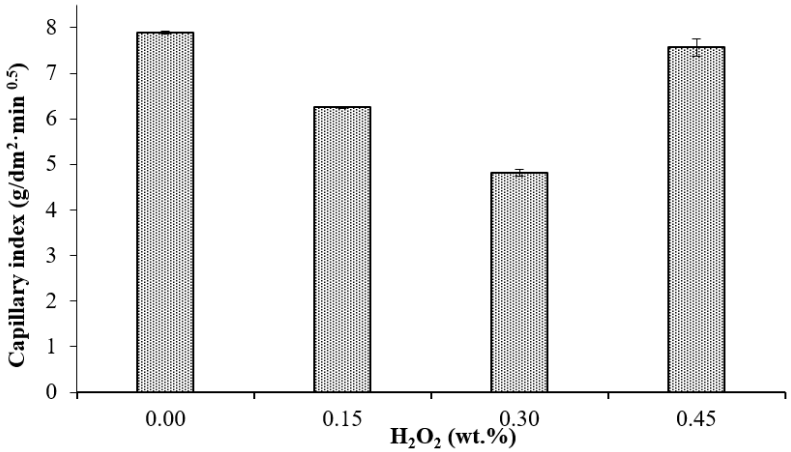

The mortar with 0.45 wt.% H_2O_2 did not follow the tendency previously observed for the mortars, showing an increase in the capillary index. This difference may be related to the amount of porogenic agent added, which caused the generation of pores with larger dimensions through the coalescence of smaller pores (Ducman and Korat, 2016), as can be observed in Fig. 23 and the pore size. This would lead to the formation of macropores in some parts of the mortars and compressing loads in other areas, thus favoring the creation of capillary pores and making it possible to increase the capillary index.

In fact, despite having similar total porosity in comparison with the composition prepared with 0.30 wt.% H_2O_2, this mortar (0.45% wt.% H_2O_2) showed much faster and greater water absorption, as demonstrated by the water absorption evolution over time, shown in Fig. 26. The water absorption for this composition reached ~ 36 %, while that observed for the mortar containing 0.30 wt.% H_2O_2 was only ~ 30 %. These results suggest that the mortars have a distinct pore size distribution, which in the case of the mortar containing a higher amount of pore forming agent resulted in a high capillary index.

Figure 26. Water absorption of mortars prepared with different hydrogen peroxide contents (wt.%).

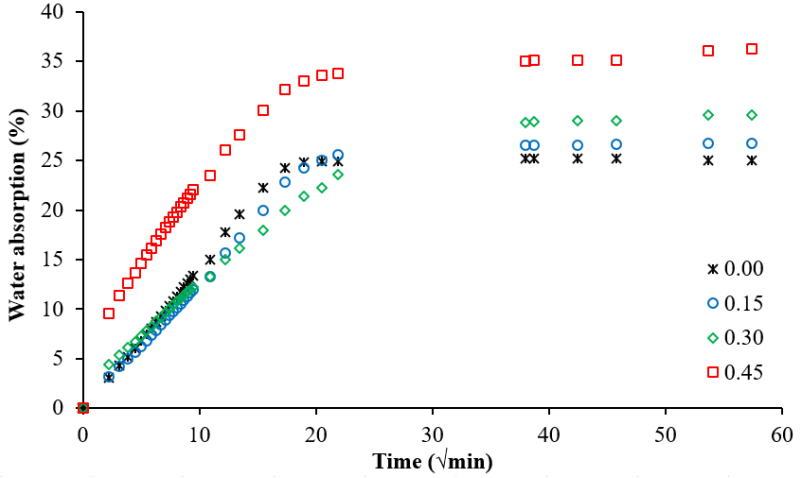

During the capillary tests, some efflorescence was observed in the mortars. One possible explanation for this is an excess of cations (Na^+ and Ca^{2+}) in the materials, as show is in the Figure 27. As the samples come into contact with water, the solubilization of salts and their migration through the pores to the surface of the mortar can occur, forming a saline deposit. It is important to note that this phenomenon of efflorescence did not occur in any of the other tests performed with the porous geopolymer mortars, for instance, in the MBV tests. Nevertheless, this effect is obviously deleterious in terms of the durability of the material and should be avoided or minimized (Vieira et al., 2014). The presence of efflorescence can be easily prevented by ensuring an appropriate mix design (e.g., decreasing the activator content), by prolonging the curing period or by curing at a slightly elevated temperature (Najafi Kani et al., 2012; Z. Zhang et al., 2014).

Figure 27. Photos of geopolymer mortar: a) without efflorescence, b) with efflorescence.

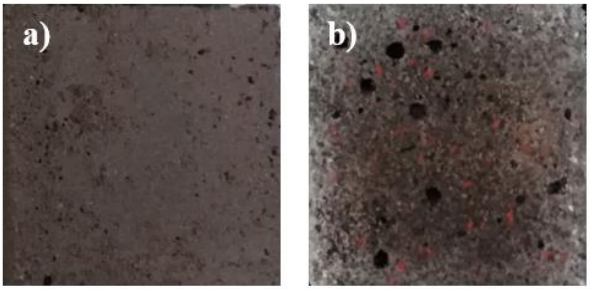

To further characterize the GMs, their thermal conductivity and apparent density were determined and the results are reported in Fig. 28. It can be observed that an increase in the concentration of porogenic agent (0.00 - 0.45 wt.%) makes the mortars lighter, with a decrease from 1.71 g/cm^3 (reference mortar) to 1.00 g/cm^3 being observed. This is associated with a reduction in the thermal conductivity of the mortars from 0.44 to 0.19 W/m·K, due to the greater amount of air trapped in the sample. This trend has been previously reported for plaster using cellulose fibers (Senff et al., 2017) and for FA-based geopolymers using hydrogen peroxide (Novais et al., 2016c) and aluminum powder (Novais et al., 2018a) as porogenic agents.

Figure 28. Thermal conductivity and apparent density of the geopolymer mortars as a function of hydrogen peroxide content.

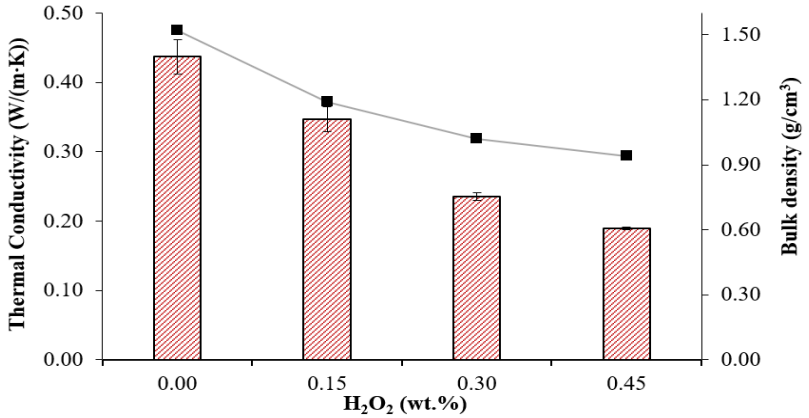

These results demonstrate the multifunctionality of the waste-based GM that may be used simultaneously as a material of low thermal conductivity (to reduce the indoor heat loss from buildings) and as an indoor moisture buffering material, thus enhancing the comfort level inside buildings and promoting energy savings.

4.3. REMARKS

The mortars were produced using a ‘green’ low-cost technology, in which an unexplored industrial waste was used as the main aluminosilicate source (biomass fly ash) and the fine aggregate was obtained from construction and demolition waste. The use of hydrogen peroxide as a porogenic agent increased the moisture buffering performance of developed geopolymer mortars. The moisture buffer values for the mortar specimens increased from 0.80 (reference mortar) to 5.61 g/m²Δ%RH (higher porosity mortar), this being the highest value ever reported for binder materials. On increasing the H_2O_2 content in the compositions there was a decrease in the thermal conductivity and mechanical performance and an increase in the water absorption and porosity. The very high moisture buffering capacity of the waste-based geopolymer mortars associated with their low thermal conductivity (0.19 W/m·K) indicates the potential for their simultaneous use for indoor moisture buffering and as a low thermal conductivity material, aimed at improving the health of the building occupants and decreasing the energy consumption associated with HVACs.

5. IN-SITU SYNTHESIS OF ZEOLITES BY GEOPOLYMERIZATION OF BIOMASS FLY ASH AND METAKAOLIN[4]

In this chapter, the in-situ synthesis of zeolites through geopolymerization of biomass fly ash wastes at low temperature in a hermetic container was evaluated. The raw materials were activated using a mixture of sodium silicate and sodium hydroxide, and then the specimens cured at 60 °C to obtain zeolite-containing geopolymers. Hydrogen peroxide (H_2O_2) was used as a porogenic agent.

Geopolymers are produced through an exothermic chemical reaction between aluminosilicate raw materials (metakaolin, fly ash, among others (Rajamma et al., 2012; Toniolo and Boccaccini, 2017) and activation solutions (mainly sodium or potassium compounds). They are regarded as amorphous materials consisting of SiO_4 and AlO_4 tetrahedral units connected by oxygens and charge-balanced by hydrated alkali cations. Those units form rings of various sizes in the network and provide the geopolymer matrix with ion exchange properties similar to those of zeolites, which show normally superior crystallinity (Papa et al., 2018).

Zeolites have been widely used as catalysts (Seo et al., 2018), ion exchangers (Tekin and Bac, 2016), molecular sieves (Gabruś et al., 2018) and adsorbents (Wang et al., 2017), since they can encapsulate in their structure a large number of small molecules (Papa et al., 2018). Among their characteristics, the zeolites usually have fixed-sized pores, allowing the filtration of some metals, giving those materials a property of selective separation of compounds (Liu et al., 2016b). Depending on the desired application, incorporation or in-situ synthesis of zeolites is essential to increase the open porosity and the surface area of the geopolymers (Zhang et al., 2016). Comparing the porous structure of both materials, the geopolymers are generally macroporous (>50 nm) and mesoporous (2 nm–50 nm), whereas the zeolites are microporous (<2 nm) (Papa et al., 2018; Takeda et al., 2013).

Many studies have been conducted to optimize the adding commercial zeolites into the geopolymer formulation (Papa et al., 2018), or by attempting to produce zeolites in-situ using hydrothermal conditions during processing (Lee et al., 2016). As examples, ZSM-20 (Minelli et al., 2016), P and X (Takeda et al., 2013), and Na-A zeolites (Greiser et

[4] Published in *Materials Letters* 236 (2019) 644-648
https://doi.org/10.1016/j.matlet.2018.11.016

al., 2017) were successfully obtained from different raw materials by geopolymerization. Geopolymer-zeolite composites also were produced by adding a zeolite as a filler to a geopolymer matrix (Liu et al., 2016a).

Thus, zeolite crystals synthesis in the structure geopolymer matrix increases the potential for use in filtration membranes, combining the geopolymer mechanical strength and the zeolite adsorptivity. In the present work, a mixture of biomass fly ash waste (75 wt.%) and metakaolin (25 wt.%) were alkali activated and cured in a hermetic container set in a heating chamber to obtain zeolite-containing geopolymers.

5.1. EXPERIMENTAL

The main objective of this work was to evaluate the effect of hydrothermal (H) conditions over time on the mineralogical characteristics of the geopolymer. Thus, a standard formulation was used, 75 wt.% BA and 25 wt.% MK (De Rossi et al., 2018), with curing of 3, 7 and 28 days (H3, H7 and H28 respectively) in hermetic glass container at 60 °C and the results obtained were compared to cure by 28 days at room temperature (R28). Based on the results achieved, other samples were prepared with addition of H_2O_2, at two different concentrations, 0.15 and 0.30 wt.% with curing of 28 days (H28-15 and H28-30, respectively).

The solids were mixed for 1 min at 60 rpm in a planetary mixer (Kenwood) and then the alkaline activators were added under the same agitation for 10 min. Stirring was continued for further 5 min at 95 rpm with addition of the H_2O_2, when necessary. The geopolymer paste was molded into cylindrical (20 mm diameter; 40 mm height) samples and cured at room temperature for 24 h in sealed plastic bags. Then, they were demolded and cured as described above. Previous tests were performed under different temperatures, and 60 °C was selected as the lowest temperature at which zeolites crystals were formed.

5.2. RESULTS AND DISCUSSION

XRD patterns of BA and MK (Fig. 29) detected calcite crystalline phases for BA and muscovite for MK, in addition to quartz in both materials. Moreover, XRD of MK showed the characteristic “hump” centered at approximately 23° 2θ. The shift of this hump to 2θ angles between 25° and 35° corresponds to a new amorphous material formation; in this case, the geopolymer gel (Davidovits and Quentin, 1991; P. Duxson et al., 2007; Novais et al., 2016b).

This hump decreases with the time that the samples stay in the heating chamber, particularly for H3 and H7 it is barely perceptible after 28 days of cure. This change is related to the conversion of geopolymer gel into crystalline zeolites. The formation of faujasite (PDF-04-014-0612) and P zeolites (PDF 00-040-1464) was observed for samples coded as H3 and H7. However, higher curing times (28 days) were found to promote an increase in the intensity of those peaks. The tests with porogenic agent (H28-15 and H28-30) were evaluated only with 28 days of cure, and the formation of characteristic peaks of sodium faujasite and P zeolites were observed. Residual quartz peaks (PDF-00-046-1045) from BA and MK were also found in all samples.

When comparing the X-ray diffractograms of raw materials with geopolymers cured under room (R28) or hydrothermal conditions (H), it can be seen that R28 still has residual peaks of muscovite (PDF-00-05-2035) and calcite (PDF-04-012-0489), as stable and less reactive crystalline phases. However, increasing the curing time of the samples in the heating chamber decreases those peaks and increases the intensity of the faujasite peaks.

Figure 29. XRD patterns of raw materials metakaolin (MK) and biomass fly ash (BA); and hydrothermal geopolymers cured for 3, 7 e 28 days (H3, H7, H28), with 0.15 or 0.30 wt.% porogenic agent (H28-15, H28-30), respectively, compared to geopolymers cured at room temperature for 28 days (R28).

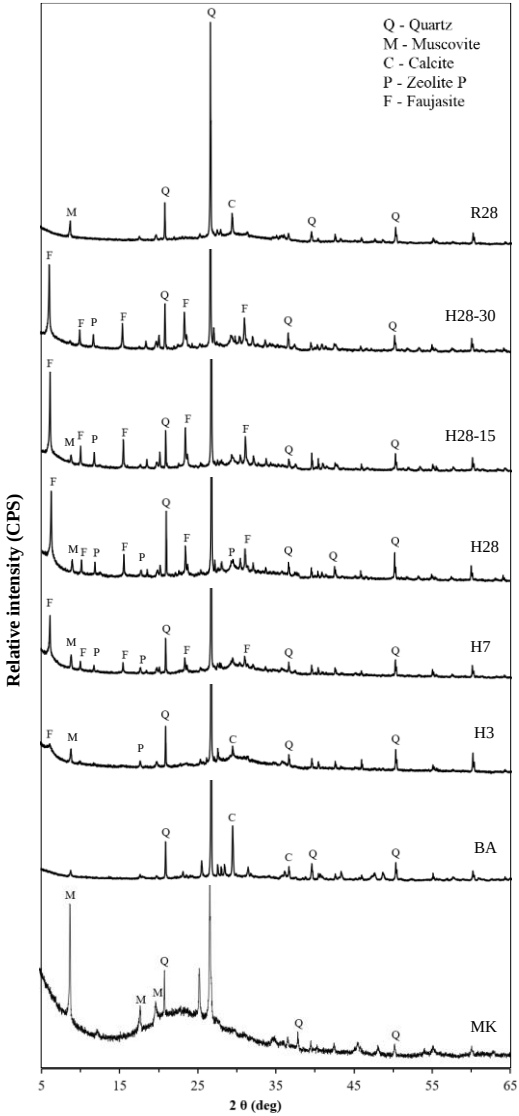

The temperature and pressure provide appropriate conditions to destabilize the crystalline structures and make them reactive to the geopolymerization process. This process of alkaline activation of crystalline materials is also referred in the literature, under specific compositional and processing conditions (Aboulayt et al., 2017; Cwirzen et al., 2014; Yip et al., 2008).

The obtained SEM microstructures (Fig. 30) were consistent with previous referred works. The P zeolite crystals appear in octahedral crystalline shape with sizes of ~1 μm [8], (Liu et al., 2016a). Moreover, H28 sample presents different crystal shapes when compared to the other samples (diamond-like and sharp edges) coherent with to those of the P zeolites found in the literature (Liu et al., 2016a). In fact, some peaks of P zeolite (PDF 00-040-1464) were identified in the H28 diffractogram, confirming that the absence of porogenic agent favored the formation of this zeolite type. In the micrographs of samples cured under room conditions (R28), it can be observed that the formed geopolymer at 100× magnification (Fig. 30a) is similar to that obtained upon curing under hydrothermal conditions (H28), with a homogeneous surface. This homogeneous surface is maintained at room temperature and can be observed in the SEM images at 500× and 2000× (Fig. 30b and 30c), while hydrothermal samples show faujasite and P zeolites crystals, as described elsewhere (Aboulayt et al., 2017; Liu et al., 2016a).

Figure 30. SEM characterization of geopolymers cured after 28 days in room condition (R28), or hydrothermally at 60 °C with 0, 0.15 or 0.30 wt.% porogenic agent (H28, H28-15 and H28-30), respectively, with a) 100×, b) 500× and c) >2000× magnification.

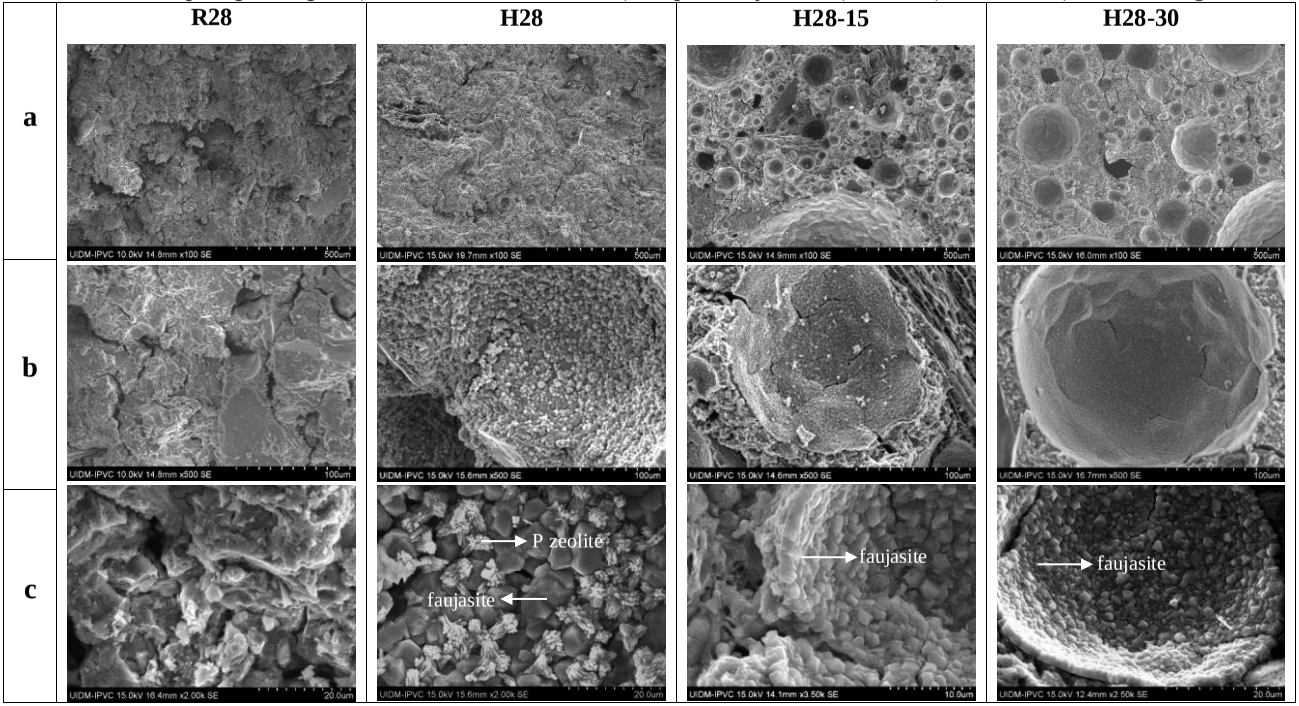

LIU et al., (2016a) and QIU et al., (2015) observed that hydrothermal conditions above 100 °C cause part of the faujasite to be converted into P zeolite. This can occur because higher temperatures increase the internal pressure in the samples favoring the formation of these crystals. In the samples obtained in the present work, the same temperature was maintained for all concentrations of porogenic agent, and only in the formulation without porogenic agent the formation of P zeolite was significant (diffraction peaks and large number of crystals in the micrographs). This can be explained by the higher internal pressure in the samples without porogenic agent (less porosity), causing the same effect reported in the literature at temperatures above 100 °C.

The bulk density results support this point, indicating that there was an increase in packing in H28 (1.16 ± 0.01 g/cm^3) compared to the values found in H28-15 (0.93 ± 0.02 g/cm^3) and H28-30 (0.75 ± 0.03 g/cm^3). This decrease in the bulk density with addition of H_2O_2 (H28-30 has a ~35% lower bulk density than H28) is associated to the closed porosity generated, as reported by Vaou and Panias (2010). The cells are normally closed and almost spherical when the percentage content of H_2O_2 is low (Vaou and Panias, 2010), as shown in the SEM images in Fig. 30a (H28-15 and H28-30).

H28 had higher apparent porosity than H28-30, Table 10. This can be explained by the formation of P zeolite in the samples without porogenic agent, increasing the apparent porosity in H28 (Zhang et al., 2016).

The porosity and density values affect directly the mechanical strength (Novais et al., 2016a), so that the higher bulk density in H28 (1.16 ± 0.01 g/cm^3) resulted in increased compressive strength (9.78 ± 0.96 MPa, Table 10). Higher amounts of porogenic agent in H28-30 decreased the bulk density (0.75 ± 0.03 g/cm^3) and the compressive strength (4.90 ± 0.45 MPa).

The mechanical strength of R28 (10.05 ± 0.17 MPa) and H28 (9.78 ± 0.96 MPa), is virtually the same, considering the dispersion of values, 1.09 ± 0.02 for R28 and 1.16 ± 0.01 g/cm^3 for H28. Here, although some works suggest an increase in mechanical strength with higher densities (Davidovits, 2008; Zhuang et al., 2016), the change in geopolymer gel microstructure into crystalline zeolites may have originated negative influences on mechanical strength, as described by De Silva and Sagoe-Crenstil, (2008).

Table 10. Mean values and standard deviation of physical properties of developed samples after 28 days curing at room (R28) or hydrothermal (H28) conditions, and with 0.15 and 0.30 wt.% porogenic agent (H28-15 and H28-30), respectively.

Properties (units)	Water absorption (%)	Apparent porosity (%)	Bulk density (g/cm^3)	Compressive strength (MPa)	BET surface area (m^2/g)
R28	42.20 ± 1.14	44.36 ± 0.95	1.09 ± 0.02	10.05 ± 0.17	40.69
H28	43.53 ± 1.17	50.38 ± 0.75	1.16 ± 0.01	9.78 ± 0.96	56.35
H28-15	50.51 ± 0.53	47.22 ± 1.23	0.93 ± 0.02	7.23 ± 0.77	-
H28-30	56.24 ± 0.54	40.73 ± 1.15	0.75 ± 0.03	4.90 ± 0.45	-

N2 adsorption and desorption isotherms (measured at 77 K) for the H28 and R28 are shown in Fig. 31, while the BET specific surface area is presented in Table 10. H28 sample exhibits Type II isotherm with a hysteresis loop typical of mesoporous materials, while R28 exhibits an isotherm characteristic of non-porous or macroporous solid, with a narrow hysteresis related to interparticle pores. In fact, this change between macro (R28) and mesoporosity (H28) corresponds to an increase of surface area (BET) from 40.69 to 56.35 m^2/g.

Figure 31. Nitrogen adsorption (circles) and desorption (diamonds) isotherms of geopolymers cured 28 days at room (R28) and hydrothermal (H28) conditions.

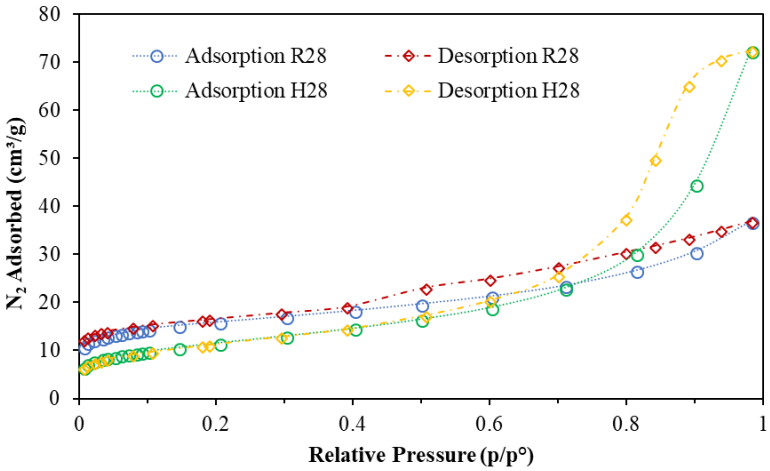

5.3. REMARKS

The results show that it is possible to obtain faujasite and P zeolites at 60 °C in sealed containers. The presence of faujasite and P zeolites was affected by the time and temperature of curing of the samples. Higher curing time (H28) intensified the XRD peaks and the amount of zeolite formed in the geopolymers. The cure in hydrothermal conditions was determinant for the development of the zeolites, since the sample cured at room temperature (R28) did not show peaks referring to zeolites.

The mechanical strength of 9.78 MPa (H28) and change of microstructure in comparison with R28 encourage the study for application of this innovative waste-based material in membranes. The identified zeolites might be employed for the treatment of atmospheric

emissions (adsorption of volatile organic compounds or CO_2 capture) or liquid effluents (adsorption of toxic metal compounds).

6. CONCLUSIONS AND OUTLOOK

The main conclusions of this thesis are:

- Geopolymers obtained from industrial waste are an alternative to ordinary Portland cement, because they reduce the environmental impact of the extraction of natural materials and the emission of CO_2, besides adding value to the wastes;
- Biomass fly ash is an efficient binder to replace metakaolin in the production of geopolymers, in amounts up to 75 wt.% of the natural raw material;
- Construction and demolition waste can be used as a fine aggregate in the production of geopolymer mortars for improving their mechanical strength;
- Geopolymers cured under environmental conditions presented similar properties to the those subjected to (hydro)thermal treatments, proving the possibilities of their in-situ industrial applications;
- Dense geopolymer mortars with high mechanical strength were developed using recycled aggregate for replacing natural aggregates, with cure under environmental conditions;
- Faujasite and P zeolites were obtained through the geopolymerization of biomass ash and metakaolin at 60 °C in sealed containers;
- Porous geopolymer mortars developed with addition of 0.45 wt.% H_2O_2 presented the highest moisture adsorption/ desorption values so far reported in the literature.

For future work, some suggestions are proposed:

- Evaluate the influence of different concentrations of sodium hydroxide to produce geopolymers;
- Investigate other waste materials for total metakaolin replacement;
- Evaluate the production of geopolymer concrete from construction and demolition waste;
- Optimize the in-situ production of zeolites in geopolymers and apply them in the treatment of liquid and gaseous effluents;
- Test new applications for geopolymers.

7. REFERENCES

ABNT:NBR 10004, 2004. Resíduos sólidos–Classificação Associação Brasileira de Normas Técnicas.

Aboulayt, A., Riahi, M., Ouazzani Touhami, M., Hannache, H., Gomina, M., Moussa, R., 2017. Properties of metakaolin based geopolymer incorporating calcium carbonate. Adv. Powder Technol. 28, 2393–2401. https://doi.org/10.1016/j.apt.2017.06.022.

Abrecon, 2015. Relatorio Pesquisa Setorial 2014/2015 [WWW Document]. Assoc. Bras. para Reciclagem Residuos da Construção Civ. e Demolição.

Adam, A.A., Horianto, X.X.X., 2014. The Effect of Temperature and Duration of Curing on the Strength of Fly Ash Based Geopolymer Mortar. Procedia Eng. 95, 410–414. https://doi.org/10.1016/j.proeng.2014.12.199.

Ahn, J., Kim, W.-S., Um, W., 2019. Development of metakaolin-based geopolymer for solidification of sulfate-rich HyBRID sludge waste. J. Nucl. Mater. 518, 247–255. https://doi.org/10.1016/j.jnucmat.2019.03.008.

Al-Kassir, A., Gañán-Gómez, J., Mohamad, A.A., Cuerda-Correa, E.M., 2010. A study of energy production from cork residues: Sawdust, sandpaper dust and triturated wood. Energy 35, 382–386. https://doi.org/10.1016/j.energy.2009.10.005.

Al Saadi, T.H.A., Badanoiu, A.I., Nicoara, A.I., Stoleriu, S., Voicu, G., 2017. Synthesis and properties of alkali activated borosilicate inorganic polymers based on waste glass. Constr. Build. Mater. 136, 298–306. https://doi.org/10.1016/j.conbuildmat.2017.01.026.

Alomayri, T., Shaikh, F.U.A., Low, I.M., 2013. Thermal and mechanical properties of cotton fabric-reinforced geopolymer composites. J. Mater. Sci. 48, 6746–6752. https://doi.org/10.1007/s10853-013-7479-2.

Arenas, C., Luna-Galiano, Y., Leiva, C., Vilches, L.F., Arroyo, F., Villegas, R., Fernández-Pereira, C., 2017. Development of a fly ash-based geopolymeric concrete with construction and demolition wastes as aggregates in acoustic barriers. Constr. Build. Mater. 134, 433–442. https://doi.org/10.1016/j.conbuildmat.2016.12.119.

Badanoiu, A.I., Al Saadi, T.H.A., Stoleriu, S., Voicu, G., 2015.

Preparation and characterization of foamed geopolymers from waste glass and red mud. Constr. Build. Mater. 84, 284–293. https://doi.org/10.1016/j.conbuildmat.2015.03.004.

Bagheri, A., Nazari, A., Hajimohammadi, A., Sanjayan, J.G., Rajeev, P., Nikzad, M., Ngo, T., Mendis, P., 2018. Microstructural study of environmentally friendly boroaluminosilicate geopolymers. J. Clean. Prod. 189, 805–812. https://doi.org/10.1016/j.jclepro.2018.04.034.

Bai, C., Li, H., Bernardo, E., Colombo, P., 2019. Waste-to-resource preparation of glass-containing foams from geopolymers. Ceram. Int. 45, 7196–7202. https://doi.org/10.1016/j.ceramint.2018.12.227.

Bakharev, T., 2005. Geopolymeric materials prepared using Class F fly ash and elevated temperature curing. Cem. Concr. Res. 35, 1224–1232. https://doi.org/10.1016/j.cemconres.2004.06.031.

Bakharev, T., Sanjayan, J.G., Cheng, Y.-B., 1999. Alkali activation of Australian slag cements. Cem. Concr. Res. 29, 113–120. https://doi.org/10.1016/S0008-8846(98)00170-7.

Braga, M., de Brito, J., Veiga, R., 2014. Reduction of the cement content in mortars made with fine concrete aggregates. Mater. Struct. 47, 171–182. https://doi.org/10.1617/s11527-013-0053-1.

Brown, R.C., Dykstra, J., 1995. Systematic errors in the use of loss-on-ignition to measure unburned carbon in fly ash. Fuel 74, 570–574. https://doi.org/10.1016/0016-2361(95)98360-Q.

Brunauer, S., Deming, L.S., Deming, W.E., Teller, E., 1940. On a Theory of the van der Waals Adsorption of Gases. J. Am. Chem. Soc. 62, 1723–1732. https://doi.org/10.1021/ja01864a025.

Chen, C., Habert, G., Bouzidi, Y., Jullien, A., 2010. Environmental impact of cement production: detail of the different processes and cement plant variability evaluation. J. Clean. Prod. 18, 478–485. https://doi.org/10.1016/j.jclepro.2009.12.014.

Cheng, T.W., Chiu, J.P., 2003. Fire-resistant geopolymer produced by granulated blast furnace slag. Miner. Eng. 16, 205–210. https://doi.org/10.1016/S0892-6875(03)00008-6.

Collins, F., Sanjayan, J., 2002. Development of Novel Alkali Activated Slag Binders to Achieve High Early Strength Concrete for Construction Use. Aust. Civ. Eng. Trans. 44, 91–102.

CONAMA, 2002. Resolução 307. Brazil.

Contreras, M., Teixeira, S.R., Lucas, M.C., Lima, L.C.N., Cardoso, D.S.L., da Silva, G.A.C., Gregório, G.C., de Souza, A.E., dos Santos, A., 2016. Recycling of construction and demolition waste for producing new construction material (Brazil case-study). Constr. Build. Mater. 123, 594–600. https://doi.org/10.1016/j.conbuildmat.2016.07.044

Criado, M., Palomo, A., Fernandez Jimenez, A., 2005. Alkali activation of fly ashes. Part 1: Effect of curing conditions on the carbonation of the reaction products. Fuel 84, 2048–2054. https://doi.org/10.1016/j.fuel.2005.03.030.

Cristelo, N., Fernández-Jiménez, A., Vieira, C., Miranda, T., Palomo, Á., 2018. Stabilisation of construction and demolition waste with a high fines content using alkali activated fly ash. Constr. Build. Mater. 170, 26–39. https://doi.org/10.1016/j.conbuildmat.2018.03.057.

Cwirzen, A., Provis, J.L., Penttala, V., Habermehl-Cwirzen, K., 2014. The effect of limestone on sodium hydroxide-activated metakaolin-based geopolymers. Constr. Build. Mater. 66, 53–62. https://doi.org/10.1016/j.conbuildmat.2014.05.022.

Davidovits, J., 2008. Geopolymer: Chemistry & Applications.

Davidovits, J., 1994. Properties of geopolymer cements, in: Proceedings First International Conference on Alkaline Cements and Concrets. Kiev-Ukraine, pp. 131–149.

Davidovits, J., 1991. Geopolymers - Inorganic polymeric new materials. J. Therm. Anal. 37, 1633–1656. https://doi.org/10.1007/BF01912193.

Davidovits, J., Quentin, S., 1991. GEOPOLYMERS Inorganic polymerie new materials. J. Therm. Anal. 37, 1633–1656. https://doi.org/10.1007/BF01912193.

De Jong, B.H.W.S., Brown, G.E., 1980. Polymerization of silicate and aluminate tetrahedra in glasses, melts, and aqueous solutions-I. Electronic structure of H6Si2O7, H6AlSiO71-, and H6Al2O72-. Geochim. Cosmochim. Acta 44, 491–511. https://doi.org/10.1016/0016-7037(80)90046-0.

De Rossi, A., Carvalheiras, J., Novais, R.M., Ribeiro, M.J., Labrincha, J.A., Hotza, D., Moreira, R.F.P.M., 2018. Waste-based geopolymeric mortars with very high moisture buffering capacity. Constr. Build. Mater. 191, 39–46. https://doi.org/10.1016/j.conbuildmat.2018.09.201.

De Rossi, A., Simão, L., Ribeiro, M.J., Novais, R.M., Labrincha, J.A., Hotza, D., Moreira, R.F.P.M., 2019. In-situ synthesis of zeolites by geopolymerization of biomass fly ash and metakaolin. Mater. Lett. 236, 644–648. https://doi.org/10.1016/j.matlet.2018.11.016.

De Silva, P., Sagoe-Crenstil, K., 2008. Medium-term phase stability of Na2O–Al2O3–SiO2–H2O geopolymer systems. Cem. Concr. Res. 38, 870–876. https://doi.org/10.1016/j.cemconres.2007.10.003.

Di Giuseppe, E., D'Orazio, M., 2014. Moisture Buffering "Active" Devices for Indoor Humidity Control: Preliminary Experimental Evaluations. Energy Procedia 62, 42–51. https://doi.org/10.1016/j.egypro.2014.12.365.

Directive 2008/98/EC, 2008. Directive 2008/98/EC of the European Parliament and of the Council of 19 November 2008 on waste and repealing certain Directives - Official J. Eur. Union - L.312/3.

Dong, M., Feng, W., Elchalakani, M., Li, G. (Kevin), Karrech, A., May, E.F., 2017. Development of a High Strength Geopolymer by Novel Solar Curing. Ceram. Int. 43, 11233–11243. https://doi.org/10.1016/j.ceramint.2017.05.173.

Duan, P., Yan, C., Zhou, W., 2017. Compressive strength and microstructure of fly ash based geopolymer blended with silica fume under thermal cycle. Cem. Concr. Compos. 78, 108–119. https://doi.org/10.1016/j.cemconcomp.2017.01.009.

Ducman, V., Korat, L., 2016. Characterization of geopolymer fly-ash based foams obtained with the addition of Al powder or H2O2 as foaming agents. Mater. Charact. 113, 207–213. https://doi.org/10.1016/j.matchar.2016.01.019.

Duxson, P., Fernández-Jiménez, A., Provis, J.L., Lukey, G.C., Palomo, A., van Deventer, J.S.J., 2007. Geopolymer technology: the current state of the art. J. Mater. Sci. 42, 2917–2933. https://doi.org/10.1007/s10853-006-0637-z.

Duxson, P., Provis, J.L., Lukey, G.C., Mallicoat, S.W., Kriven, W.M., Van Deventer, J.S.J., 2005. Understanding the relationship between geopolymer composition, microstructure and mechanical properties. Colloids Surfaces A Physicochem. Eng. Asp. 269, 47–58. https://doi.org/10.1016/j.colsurfa.2005.06.060.

Duxson, Peter, Provis, J.L., Lukey, G.C., van Deventer, J.S.J., 2007. The role of inorganic polymer technology in the development of 'green concrete.' Cem. Concr. Res. 37, 1590–1597. https://doi.org/10.1016/j.cemconres.2007.08.018.

EN 998-2, 2010. Specification for mortar for masonry - Part 2: Masonry mortar.

European Commission, 2001. Competitiveness of the Construction Industry, A Report Drawn up by the Working Group for Sustainable Construction with Participants from the European Commission, Member States and Industry.

European Commission, 2000. European List of Wastes, Commission Decision 2000/532/EC.

Eutostat, 2014. Environment and Energy [WWW Document]. Gener. Treat. waste. URL http://ec.europa.eu/eurostat/ (accessed 2.13.18).

Fan, C.-C., Huang, R., Hwang, H., Chao, S.-J., 2015. The Effects of Different Fine Recycled Concrete Aggregates on the Properties of Mortar. Materials (Basel). 8, 2658–2672. https://doi.org/10.3390/ma8052658.

Fernández-Pereira, C., Luna-Galiano, Y., Pérez-Clemente, M., Leiva, C., Arroyo, F., Villegas, R., Vilches, L.F., 2018. Immobilization of heavy metals (Cd, Ni or Pb) using aluminate geopolymers. Mater. Lett. 227, 184–186. https://doi.org/10.1016/j.matlet.2018.05.027.

Gabruś, E., Witkiewicz, K., Nastaj, J., 2018. Modeling of regeneration stage of 3A and 4A zeolite molecular sieves in TSA process used for dewatering of aliphatic alcohols. Chem. Eng. J. 337, 416–427. https://doi.org/10.1016/j.cej.2017.12.112.

Gianangeli, A., Di Giuseppe, E., D'Orazio, M., 2017. Design and performance assessment of building counter-walls integrating Moisture Buffering "active" devices. Energy Procedia 132, 105–110. https://doi.org/10.1016/j.egypro.2017.09.652.

Giasuddin, H.M., Sanjayan, J.G., Ranjith, P.G., 2013. Strength of geopolymer cured in saline water in ambient conditions. Fuel 107, 34–39. https://doi.org/10.1016/j.fuel.2013.01.035.

Giosuè, C., Mobili, A., Toscano, G., Ruello, M.L., Tittarelli, F., 2016. Effect of Biomass Waste Materials as Unconventional Aggregates in Multifunctional Mortars for Indoor Application. Procedia Eng. 161, 655–659. https://doi.org/10.1016/j.proeng.2016.08.724.

Gomes, M.G., Flores-Colen, I., Manga, L.M., Soares, A., de Brito, J., 2017. The influence of moisture content on the thermal conductivity of external thermal mortars. Constr. Build. Mater. 135, 279–286. https://doi.org/10.1016/j.conbuildmat.2016.12.166.

Gonçalves, H., Gonçalves, B., Silva, L., Raupp-Pereira, F., Senff, L., Labrincha, J.A., 2014a. Development of porogene-containing mortars for levelling the indoor ambient moisture. Ceram. Int. 40, 15489–15495. https://doi.org/10.1016/j.ceramint.2014.07.010.

Gonçalves, H., Gonçalves, B., Silva, L., Vieira, N., Raupp-Pereira, F., Senff, L., Labrincha, J.A., 2014b. The influence of porogene additives on the properties of mortars used to control the ambient moisture. Energy Build. 74, 61–68. https://doi.org/10.1016/j.enbuild.2014.01.016

González, J.F., Ledesma, B., Alkassir, A., González, J., 2011. Study of the influence of the composition of several biomass pellets on the drying process. Biomass and Bioenergy 35, 4399–4406. https://doi.org/10.1016/j.biombioe.2011.08.019.

Greiser, S., Sturm, P., Gluth, G.J.G., Hunger, M., Jäger, C., 2017. Differentiation of the solid-state NMR signals of gel, zeolite phases and water species in geopolymer-zeolite composites. Ceram. Int. 43, 2202–2208. https://doi.org/10.1016/j.ceramint.2016.11.004.

Gunasekara, C., Law, D., Bhuiyan, S., Setunge, S., Ward, L., 2019. Chloride induced corrosion in different fly ash based geopolymer concretes. Constr. Build. Mater. 200, 502–513. https://doi.org/10.1016/j.conbuildmat.2018.12.168.

Hameury, S., 2005. Moisture buffering capacity of heavy timber structures directly exposed to an indoor climate: a numerical study. Build. Environ. 40, 1400–1412. https://doi.org/10.1016/j.buildenv.2004.10.017.

Hameury, S., Lundström, T., 2004. Contribution of indoor exposed massive wood to a good indoor climate: in situ measurement campaign. Energy Build. 36, 281–292. https://doi.org/10.1016/j.enbuild.2003.12.003.

Hardjito, D., Rangan, B. V., 2005. Development and properties of low-calcium fly ash-based geopoloymer concrete. Perth, Australia.

Hassan, A., Arif, M., Shariq, M., 2019. Use of geopolymer concrete for a cleaner and sustainable environment – A review of mechanical properties and microstructure. J. Clean. Prod. 223, 704–728.

https://doi.org/10.1016/j.jclepro.2019.03.051.

Haykırı-Açma, H., 2003. Combustion characteristics of different biomass materials. Energy Convers. Manag. 44, 155–162. https://doi.org/10.1016/S0196-8904(01)00200-X.

Hertel, T., Novais, R.M., Alarcón, R.M., Labrincha, J.A., Pontikes, Y., 2019. Use of modified bauxite residue-based porous inorganic polymer monoliths as adsorbents of methylene blue. J. Clean. Prod. https://doi.org/10.1016/j.jclepro.2019.04.084.

Huntzinger, D.N., Eatmon, T.D., 2009. A life-cycle assessment of Portland cement manufacturing: comparing the traditional process with alternative technologies. J. Clean. Prod. 17, 668–675. https://doi.org/10.1016/j.jclepro.2008.04.007.

Huseien, G.F., Ismail, M., Khalid, N.H.A., Hussin, M.W., Mirza, J., 2018. Compressive strength and microstructure of assorted wastes incorporated geopolymer mortars: Effect of solution molarity. Alexandria Eng. J. 57, 3375–3386. https://doi.org/10.1016/j.aej.2018.07.011.

Hwang, E.-H., Ko, Y.S., Jeon, J.-K., 2008. Effect of polymer cement modifiers on mechanical and physical properties of polymer-modified mortar using recycled artificial marble waste fine aggregate. J. Ind. Eng. Chem. 14, 265–271. https://doi.org/10.1016/j.jiec.2007.11.002.

ISO 24353, 2008. Hygrothermal performance of building materials and products- Determination of moisture adsorption/desorption properties in response to humidity variation.

Izquierdo, M., Querol, X., Phillipart, C., Antenucci, D., Towler, M., 2010. The role of open and closed curing conditions on the leaching properties of fly ash-slag-based geopolymers. J. Hazard. Mater. 176, 623–628. https://doi.org/10.1016/j.jhazmat.2009.11.075.

Jiménez, J.R., Ayuso, J., López, M., Fernández, J.M., de Brito, J., 2013. Use of fine recycled aggregates from ceramic waste in masonry mortar manufacturing. Constr. Build. Mater. 40, 679–690. https://doi.org/10.1016/j.conbuildmat.2012.11.036.

Jin, M., Lian, F., Xia, R., Wang, Z., 2018. Formulation and durability of a geopolymer based on metakaolin/tannery sludge. Waste Manag. 79, 717–728. https://doi.org/10.1016/j.wasman.2018.08.039.

Khale, D., Chaudhary, R., 2007. Mechanism of geopolymerization and factors influencing its development: a review. J. Mater. Sci. 42, 729–746.

https://doi.org/10.1007/s10853-006-0401-4.

Khalid, H.R., Lee, N.K., Park, S.M., Abbas, N., Lee, H.K., 2018. Synthesis of geopolymer-supported zeolites via robust one-step method and their adsorption potential. J. Hazard. Mater. 353, 522–533. https://doi.org/10.1016/j.jhazmat.2018.04.049.

Komnitsas, K., Zaharaki, D., Vlachou, A., Bartzas, G., Galetakis, M., 2015. Effect of synthesis parameters on the quality of construction and demolition wastes (CDW) geopolymers. Adv. Powder Technol. 26, 368–376. https://doi.org/10.1016/j.apt.2014.11.012.

Kong, D.L.Y., Sanjayan, J.G., Sagoe-Crentsil, K., 2008. Factors affecting the performance of metakaolin geopolymers exposed to elevated temperatures. J. Mater. Sci. 43, 824–831. https://doi.org/10.1007/s10853-007-2205-6.

Koshy, N., Dondrob, K., Hu, L., Wen, Q., Meegoda, J.N., 2019. Synthesis and characterization of geopolymers derived from coal gangue, fly ash and red mud. Constr. Build. Mater. 206, 287–296. https://doi.org/10.1016/j.conbuildmat.2019.02.076.

Lagaly, G., Tufar, W., Minihan, A., Lovell, A., 2000. Silicates, in: Ullmann's Encyclopedia of Industrial Chemistry. Wiley-VCH Verlag GmbH & Co. KGaA, Weinheim, Germany. https://doi.org/10.1002/14356007.a23_661.

Lahoti, M., Yang, E.-H., Tan, K.H., 2017. Influence of Mix Design Parameters on Geopolymer Mechanical Properties and Microstructure. pp. 21–33. https://doi.org/10.1002/9781119321811.ch3.

Le, T., Wang, Q., Ravindra, A.V., Li, X., Ju, S., 2019. Microwave intensified synthesis of Zeolite-Y from spent FCC catalyst after acid activation. J. Alloys Compd. 776, 437–446. https://doi.org/10.1016/j.jallcom.2018.10.316.

Ledesma, E.F., Jiménez, J.R., Ayuso, J., Fernández, J.M., de Brito, J., 2015. Maximum feasible use of recycled sand from construction and demolition waste for eco-mortar production – Part-I: ceramic masonry waste. J. Clean. Prod. 87, 692–706. https://doi.org/10.1016/j.jclepro.2014.10.084.

Lee, N.K., Khalid, H.R., Lee, H.K., 2016. Synthesis of mesoporous geopolymers containing zeolite phases by a hydrothermal treatment. Microporous Mesoporous Mater. 229, 22–30.

https://doi.org/10.1016/j.micromeso.2016.04.016.

Lee, W.-H., Cheng, T.-W., Ding, Y.-C., Lin, K.-L., Tsao, S.-W., Huang, C.-P., 2019. Geopolymer technology for the solidification of simulated ion exchange resins with radionuclides. J. Environ. Manage. 235, 19–27. https://doi.org/10.1016/j.jenvman.2019.01.027.

Leong, H.Y., Ong, D.E.L., Sanjayan, J.G., Nazari, A., 2016. The effect of different Na 2 O and K 2 O ratios of alkali activator on compressive strength of fly ash based-geopolymer. Constr. Build. Mater. 106, 500–511. https://doi.org/10.1016/j.conbuildmat.2015.12.141.

Liguori, B., Capasso, I., De Pertis, M., Ferone, C., Cioffi, R., 2017. Geopolymerization Ability of Natural and Secondary Raw Materials by Solubility Test in Alkaline Media. Environments 4, 56. https://doi.org/10.3390/environments4030056.

Liu, Y., Yan, C., Qiu, X., Li, D., Wang, H., Alshameri, A., 2016a. Preparation of faujasite block from fly ash-based geopolymer via in-situ hydrothermal method. J. Taiwan Inst. Chem. Eng. 59, 433–439. https://doi.org/10.1016/j.jtice.2015.07.012.

Liu, Y., Yan, C., Zhang, Z., Wang, H., Zhou, S., Zhou, W., 2016b. A comparative study on fly ash, geopolymer and faujasite block for Pb removal from aqueous solution. Fuel 185, 181–189. https://doi.org/10.1016/j.fuel.2016.07.116.

Loo, S. van, Koppejan, J., 2008. Handbook of biomass combustion and co-firing, 2nd ed. Earthscan, London, UK.

Maleki, A., Hajizadeh, Z., Sharifi, V., Emdadi, Z., 2019. A green, porous and eco-friendly magnetic geopolymer adsorbent for heavy metals removal from aqueous solutions. J. Clean. Prod. 215, 1233–1245. https://doi.org/10.1016/j.jclepro.2019.01.084.

Martínez, I., Etxeberria, M., Pavón, E., Díaz, N., 2013. A comparative analysis of the properties of recycled and natural aggregate in masonry mortars. Constr. Build. Mater. 49, 384–392. https://doi.org/10.1016/j.conbuildmat.2013.08.049.

McLellan, B.C., Williams, R.P., Lay, J., van Riessen, A., Corder, G.D., 2011. Costs and carbon emissions for geopolymer pastes in comparison to ordinary portland cement. J. Clean. Prod. 19, 1080–1090. https://doi.org/10.1016/j.jclepro.2011.02.010.

Mehta, A., Siddique, R., 2017. Strength, permeability and micro-

structural characteristics of low-calcium fly ash based geopolymers. Constr. Build. Mater. 141, 325–334. https://doi.org/10.1016/j.conbuildmat.2017.03.031.

Mermerdaş, K., Algın, Z., Oleiwi, S.M., Nassani, D.E., 2017a. Optimization of lightweight GGBFS and FA geopolymer mortars by response surface method. Constr. Build. Mater. 139, 159–171. https://doi.org/10.1016/j.conbuildmat.2017.02.050.

Mermerdaş, K., Manguri, S., Nassani, D.E., Oleiwi, S.M., 2017b. Effect of aggregate properties on the mechanical and absorption characteristics of geopolymer mortar. Eng. Sci. Technol. an Int. J. 20, 1642–1652. https://doi.org/10.1016/j.jestch.2017.11.009.

Meyer, C., 2009. The greening of the concrete industry. Cem. Concr. Compos. 31, 601–605. https://doi.org/10.1016/j.cemconcomp.2008.12.010.

Minelli, M., Medri, V., Papa, E., Miccio, F., Landi, E., Doghieri, F., 2016. Geopolymers as solid adsorbent for CO2 capture. Chem. Eng. Sci. 148, 267–274. https://doi.org/10.1016/j.ces.2016.04.013.

Miranda, L.F.R., Angulo, S.C., Careli, É.D., 2009. A reciclagem de resíduos de construção e demolição no Brasil: 1986-2008. Ambient. Construído 9, 57–71.

Miranda, L.F.R., TORRES, L., Vogt, V., BROCARDO, F.L.M., Bartoli, H., 2016. Panorama atual do setor de reciclagem de resíduos de construção e demolição no Brasil, in: XVI Encontro Nacional de Tecnologia Do Ambiente Construído. São Paulo - Brazil, p. 21.

Modolo, R.C.E., Tarelho, L.A.C., Teixeira, E.R., Ferreira, V.M., Labrincha, J.A., 2014. Treatment and use of bottom bed waste in biomass fluidized bed combustors. Fuel Process. Technol. 125, 170–181. https://doi.org/10.1016/j.fuproc.2014.03.040.

Mohammadinia, A., Arulrajah, A., Sanjayan, J., Disfani, M.M., Win Bo, M., Darmawan, S., 2016. Stabilization of Demolition Materials for Pavement Base/Subbase Applications Using Fly Ash and Slag Geopolymers: Laboratory Investigation. J. Mater. Civ. Eng. 28, 04016033. https://doi.org/10.1061/(ASCE)MT.1943-5533.0001526.

Mohseni, E., 2018. Assessment of Na2SiO3 to NaOH ratio impact on the performance of polypropylene fiber-reinforced geopolymer composites. Constr. Build. Mater. 186, 904–911.

https://doi.org/10.1016/j.conbuildmat.2018.08.032.

Mohseni, E., Naseri, F., Amjadi, R., Khotbehsara, M.M., Ranjbar, M.M., 2016. Microstructure and durability properties of cement mortars containing nano-TiO 2 and rice husk ash. Constr. Build. Mater. 114, 656–664. https://doi.org/10.1016/j.conbuildmat.2016.03.136.

Moreno, R., 2005. Reologia de suspensiones cerâmicas. Consejo Superior de Investigaciones Científicas, Spain.

Mustafa Al Bakri, A.M., Kamarudin, H., Bnhussain, M., Nizar, I.K., Rafiza, A.R., Zarina, Y., 2012. The processing, characterization, and properties of fly ash based geopolymer concrete. Rev. Adv. Mater. Sci. 30, 90–97.

Najafi Kani, E., Allahverdi, A., Provis, J.L., 2012. Efflorescence control in geopolymer binders based on natural pozzolan. Cem. Concr. Compos. 34, 25–33. https://doi.org/10.1016/j.cemconcomp.2011.07.007.

Narayanan, A., Shanmugasundaram, P., 2017. An Experimental Investigation on Flyash-based Geopolymer Mortar under different curing regime for Thermal Analysis. Energy Build. 138, 539–545. https://doi.org/10.1016/j.enbuild.2016.12.079.

Nazari, A., Khalaj, G., Riahi, S., Bohlooli, H., Kaykha, M.M., 2012. Prediction total specific pore volume of geopolymers produced from waste ashes by ANFIS. Ceram. Int. 38, 3111–3120. https://doi.org/10.1016/j.ceramint.2011.12.011.

Neno, C., Brito, J. de, Veiga, R., 2014. Using fine recycled concrete aggregate for mortar production. Mater. Res. 17, 168–177. https://doi.org/10.1590/S1516-14392013005000164

Nikolov, A., Rostovsky, I., Nugteren, H., 2017. Geopolymer materials based on natural zeolite. Case Stud. Constr. Mater. 6, 198–205. https://doi.org/10.1016/j.cscm.2017.03.001.

Novais, R.M., Ascensão, G., Buruberri, L.H., Senff, L., Labrincha, J.A., 2016a. Influence of blowing agent on the fresh- and hardened-state properties of lightweight geopolymers. Mater. Des. 108, 551–559. https://doi.org/10.1016/j.matdes.2016.07.039.

Novais, R.M., Ascensão, G., Ferreira, N., Seabra, M.P., Labrincha, J.A., 2018a. Influence of water and aluminium powder content on the properties of waste-containing geopolymer foams. Ceram. Int. 44, 6242–6249. https://doi.org/10.1016/j.ceramint.2018.01.009.

Novais, R.M., Ascensão, G., Seabra, M.P., Labrincha, J.A., 2016b. Waste glass from end-of-life fluorescent lamps as raw material in geopolymers. Waste Manag. 52, 245–255. https://doi.org/10.1016/j.wasman.2016.04.003.

Novais, R.M., Ascensão, G., Tobaldi, D.M., Seabra, M.P., Labrincha, J.A., 2018b. Biomass fly ash geopolymer monoliths for effective methylene blue removal from wastewaters. J. Clean. Prod. 171, 783–794. https://doi.org/10.1016/j.jclepro.2017.10.078.

Novais, R.M., Buruberri, L.H., Ascensão, G., Seabra, M.P., Labrincha, J.A., 2016c. Porous biomass fly ash-based geopolymers with tailored thermal conductivity. J. Clean. Prod. 119, 99–107. https://doi.org/10.1016/j.jclepro.2016.01.083.

Novais, R.M., Buruberri, L.H., Seabra, M.P., Bajare, D., Labrincha, J.A., 2016d. Novel porous fly ash-containing geopolymers for pH buffering applications. J. Clean. Prod. 124, 395–404. https://doi.org/10.1016/j.jclepro.2016.02.114.

Novais, R.M., Carvalheiras, J., Seabra, M.P., Pullar, R.C., Labrincha, J.A., 2019. Red mud-based inorganic polymer spheres bulk-type adsorbents and pH regulators. Mater. Today 23, 105–106. https://doi.org/10.1016/j.mattod.2019.01.014.

Novais, R.M., Seabra, M.P., Labrincha, J.A., 2017. Porous geopolymer spheres as novel pH buffering materials. J. Clean. Prod. 143, 1114–1122. https://doi.org/10.1016/j.jclepro.2016.12.008.

Osanyintola, O.F., Talukdar, P., Simonson, C.J., 2006. Effect of initial conditions, boundary conditions and thickness on the moisture buffering capacity of spruce plywood. Energy Build. 38, 1283–1292. https://doi.org/10.1016/j.enbuild.2006.03.024.

Ozer, I., Soyer-Uzun, S., 2015. Relations between the structural characteristics and compressive strength in metakaolin based geopolymers with different molar Si/Al ratios. Ceram. Int. 41, 10192–10198. https://doi.org/10.1016/j.ceramint.2015.04.125.

Pacheco-Torgal, F., Castro-Gomes, J., Jalali, S., 2008. Alkali-activated binders: A review. Constr. Build. Mater. 22, 1305–1314. https://doi.org/10.1016/j.conbuildmat.2007.10.015.

Pacheco-Torgal, F., Ding, Y., Miraldo, S., Abdollahnejad, Z., Labrincha, J.A., 2012. Are geopolymers more suitable than Portland cement to

produce high volume recycled aggregates HPC? Constr. Build. Mater. 36, 1048–1052. https://doi.org/10.1016/j.conbuildmat.2012.07.004.

Padfield, T.I.M., 1999. Humidity buffering of interior spaces by porous , absorbent insulation by porous , absorbent insulation 19.

Palomo, A., Grutzeck, M.W., Blanco, M.T., 1999. Alkali-activated fly ashes. Cem. Concr. Res. 29, 1323–1329. https://doi.org/10.1016/S0008-8846(98)00243-9.

Papa, E., Medri, V., Amari, S., Manaud, J., Benito, P., Vaccari, A., Landi, E., 2018. Zeolite-geopolymer composite materials: Production and characterization. J. Clean. Prod. 171, 76–84. https://doi.org/10.1016/j.jclepro.2017.09.270.

PAS 8820, 2016. Construction Materials – Alkali-Activated Cementitious Material and Concrete – Specification, BSI Standards Limited.

Provis, J.L., Bernal, S.A., 2014. Geopolymers and Related Alkali-Activated Materials. Annu. Rev. Mater. Res. 44, 299–327. https://doi.org/10.1146/annurev-matsci-070813-113515.

Provis, J.L., Lukey, G.C., van Deventer, J.S.J., 2005. Do Geopolymers Actually Contain Nanocrystalline Zeolites? A Reexamination of Existing Results. Chem. Mater. 17, 3075–3085. https://doi.org/10.1021/cm050230i.

Puertas, F., Fernández-Jiménez, A., 2003. Mineralogical and microstructural characterisation of alkali-activated fly ash/slag pastes. Cem. Concr. Compos. 25, 287–292. https://doi.org/10.1016/S0958-9465(02)00059-8.

Puertas, F., Martínez-Ramírez, S., Alonso, S., Vázquez, T., 2000. Alkali-activated fly ash/slag cements. Cem. Concr. Res. 30, 1625–1632. https://doi.org/10.1016/S0008-8846(00)00298-2.

Qiu, X., Liu, Y., Li, D., Yan, C., 2015. Preparation of NaP zeolite block from fly ash-based geopolymer via in situ hydrothermal method. J. Porous Mater. 22, 291–299. https://doi.org/10.1007/s10934-014-9895-3

Raeis Samiei, R., Daniotti, B., Pelosato, R., Dotelli, G., 2015. Properties of cement–lime mortars vs. cement mortars containing recycled concrete aggregates. Constr. Build. Mater. 84, 84–94. https://doi.org/10.1016/j.conbuildmat.2015.03.042.

Rajamma, R., Labrincha, J.A., Ferreira, V.M., 2012. Alkali activation of

biomass fly ash-metakaolin blends. Fuel 98, 265–271. https://doi.org/10.1016/j.fuel.2012.04.006.

Ramli, M.B., Alonge, O.R., 2016. Characterization of metakaolin and study on early age mechanical strength of hybrid cementitious composites. Constr. Build. Mater. 121, 599–611. https://doi.org/10.1016/j.conbuildmat.2016.06.039.

Reig, L., Sanz, M.A., Borrachero, M.V., Monzó, J., Soriano, L., Payá, J., 2017. Compressive strength and microstructure of alkali-activated mortars with high ceramic waste content. Ceram. Int. 43, 13622–13634. https://doi.org/10.1016/j.ceramint.2017.07.072.

Rode, C., Peuhkuri, R., Time, B., Svennberg, K., Ojanen, T., Mukhopadhyaya, P., Kumaran, M., Dean, S.W., 2007. Moisture Buffer Value of Building Materials. J. ASTM Int. 4, 100369. https://doi.org/10.1520/JAI100369.

Roviello, G., Ricciotti, L., Ferone, C., Colangelo, F., Tarallo, O., 2015. Fire resistant melamine based organic-geopolymer hybrid composites. Cem. Concr. Compos. 59, 89–99. https://doi.org/10.1016/j.cemconcomp.2015.03.007.

Saiz Martínez, P., González Cortina, M., Fernández Martínez, F., Rodríguez Sánchez, A., 2016. Comparative study of three types of fine recycled aggregates from construction and demolition waste (CDW), and their use in masonry mortar fabrication. J. Clean. Prod. 118, 162–169. https://doi.org/10.1016/j.jclepro.2016.01.059.

Sami, M., Annamalai, K., Wooldridge, M., 2001. Co-firing of coal and biomass fuel blends. Prog. Energy Combust. Sci. 27, 171–214. https://doi.org/10.1016/S0360-1285(00)00020-4.

Senff, L., Ascensão, G., Ferreira, V.M., Seabra, M.P., Labrincha, J.A., 2017. Development of multifunctional plaster using nano-TiO 2 and distinct particle size cellulose fibers. Energy Build. https://doi.org/10.1016/j.enbuild.2017.10.060.

Senff, L., Ascensão, G., Hotza, D., Ferreira, V.M., Labrincha, J.A., 2016. Assessment of the single and combined effect of superabsorbent particles and porogenic agents in nanotitania-containing mortars. Energy Build. 127, 980–990. https://doi.org/10.1016/j.enbuild.2016.06.048.

Senff, L., Barbetta, P.A., Repette, W.L., Hotza, D., Paiva, H., Ferreira, V.M., Labrincha, J.A., 2009. Mortar composition defined according to

rheometer and flow table tests using factorial designed experiments. Constr. Build. Mater. 23, 3107–3111. https://doi.org/10.1016/j.conbuildmat.2009.06.028.

Senff, L., Modolo, R.C.E., Ascensão, G., Hotza, D., Ferreira, V.M., Labrincha, J.A., 2015. Development of mortars containing superabsorbent polymer. Constr. Build. Mater. 95, 575–584. https://doi.org/10.1016/j.conbuildmat.2015.07.173.

Seo, D.-W., Rahma, S.T., Reddy, B.M., Park, S.-E., 2018. Carbon dioxide assisted toluene side-chain alkylation with methanol over Cs-X zeolite catalyst. J. CO2 Util. 26, 254–261. https://doi.org/10.1016/j.jcou.2018.05.001.

Silva, R.V., de Brito, J., Dhir, R.K., 2016. Performance of cementitious renderings and masonry mortars containing recycled aggregates from construction and demolition wastes. Constr. Build. Mater. 105, 400–415. https://doi.org/10.1016/j.conbuildmat.2015.12.171.

Simão, L., Jiusti, J., Lóh, N.J., Hotza, D., Raupp-Pereira, F., Labrincha, J.A., Montedo, O.R.K., 2017. Waste-containing clinkers: Valorization of alternative mineral sources from pulp and paper mills. Process Saf. Environ. Prot. 109. https://doi.org/10.1016/j.psep.2017.03.038.

Siyal, A.A., Shamsuddin, M.R., Khan, M.I., Rabat, N.E., Zulfiqar, M., Man, Z., Siame, J., Azizli, K.A., 2018. A review on geopolymers as emerging materials for the adsorption of heavy metals and dyes. J. Environ. Manage. 224, 327–339. https://doi.org/10.1016/j.jenvman.2018.07.046.

Sohn, H.Y., Moreland, C., 1968. The effect of particle size distribution on packing density. Can. J. Chem. Eng. 46, 162–167. https://doi.org/10.1002/cjce.5450460305.

Svennberg K, Hedegaard L, R.C., 2004. Moisture buffer performance of a fully furnished room. Proc. Build. IX, Clear.

Swanepoel, J.C., Strydom, C.A., 2002. Utilisation of fly ash in a geopolymeric material. Appl. Geochemistry 17, 1143–1148. https://doi.org/10.1016/S0883-2927(02)00005-7.

Takeda, H., Hashimoto, S., Yokoyama, H., Honda, S., Iwamoto, Y., 2013. Characterization of Zeolite in Zeolite-Geopolymer Hybrid Bulk Materials Derived from Kaolinitic Clays. Materials (Basel). 6, 1767–1778. https://doi.org/10.3390/ma6051767.

Tarelho, L.A.C., Coelho, A.M.S.L., Teixeira, E.R., Rajamma, R., Ferreira, V.M., 2011. Characteristics of ashes from two Portuguese biomass cogeneration plants, in: Proceedings of the 19th European Biomass Conference & Exhibition. Berlin, Germany, pp. 1041–1053.

Tarelho, L.A.C., Teixeira, E.R., Silva, D.F.R., Modolo, R.C.E., Labrincha, J.A., Rocha, F., 2015. Characteristics of distinct ash flows in a biomass thermal power plant with bubbling fluidised bed combustor. Energy 90, 387–402. https://doi.org/10.1016/j.energy.2015.07.036.

Teixeira, E.R., Camões, A., Branco, F.G., 2019. Valorisation of wood fly ash on concrete. Resour. Conserv. Recycl. 145, 292–310. https://doi.org/10.1016/j.resconrec.2019.02.028.

Tekin, R., Bac, N., 2016. Antimicrobial behavior of ion-exchanged zeolite X containing fragrance. Microporous Mesoporous Mater. 234, 55–60. https://doi.org/10.1016/j.micromeso.2016.07.006.

Tittarelli, F., Giosuè, C., Mobili, A., Ruello, M.L., 2015. Influence of binders and aggregates on VOCs adsorption and moisture buffering activity of mortars for indoor applications. Cem. Concr. Compos. 57, 75–83. https://doi.org/10.1016/j.cemconcomp.2014.11.013.

Toniolo, N., Boccaccini, A.R., 2017. Fly ash-based geopolymers containing added silicate waste . A review. Ceram. Int. 43, 14545–14551. https://doi.org/10.1016/j.ceramint.2017.07.221.

Toniolo, N., Rincón, A., Avadhut, Y.S.S., Hartmann, M., Bernardo, E., Boccaccini, A.R.R., 2018. Novel geopolymers incorporating red mud and waste glass cullet. Mater. Lett. 219, 152–154. https://doi.org/10.1016/j.matlet.2018.02.061.

Topçu, İ.B., Bilir, T., 2010. Experimental investigation of drying shrinkage cracking of composite mortars incorporating crushed tile fine aggregate. Mater. Des. 31, 4088–4097. https://doi.org/10.1016/j.matdes.2010.04.047.

Torkittikul, P., Chaipanich, A., 2010. Utilization of ceramic waste as fine aggregate within Portland cement and fly ash concretes. Cem. Concr. Compos. 32, 440–449. https://doi.org/10.1016/j.cemconcomp.2010.02.004.

Turner, L.K., Collins, F.G., 2013. Carbon dioxide equivalent (CO2-e) emissions: A comparison between geopolymer and OPC cement concrete. Constr. Build. Mater. 43, 125–130.

https://doi.org/10.1016/j.conbuildmat.2013.01.023.

Tuyan, M., Andiç-Çakir, Ö., Ramyar, K., 2018. Effect of alkali activator concentration and curing condition on strength and microstructure of waste clay brick powder-based geopolymer. Compos. Part B Eng. 135, 242–252. https://doi.org/10.1016/j.compositesb.2017.10.013.

Van Jaarsveld, J.G.., Van Deventer, J.S.., Lukey, G.., 2002. The effect of composition and temperature on the properties of fly ash- and kaolinite-based geopolymers. Chem. Eng. J. 89, 63–73. https://doi.org/10.1016/S1385-8947(02)00025-6.

Vaou, V., Panias, D., 2010. Thermal insulating foamy geopolymers from perlite. Miner. Eng. 23, 1146–1151. https://doi.org/10.1016/j.mineng.2010.07.015.

Vásquez, A., Cárdenas, V., Robayo, R.A., de Gutiérrez, R.M., 2016. Geopolymer based on concrete demolition waste. Adv. Powder Technol. 27, 1173–1179. https://doi.org/10.1016/j.apt.2016.03.029.

Vassilev, S. V., Baxter, D., Andersen, L.K., Vassileva, C.G., 2010. An overview of the chemical composition of biomass. Fuel 89, 913–933. https://doi.org/10.1016/j.fuel.2009.10.022.

Vassilev, S. V., Baxter, D., Vassileva, C.G., 2013. An overview of the behaviour of biomass during combustion: Part I. Phase-mineral transformations of organic and inorganic matter. Fuel 112, 391–449. https://doi.org/10.1016/j.fuel.2013.05.043.

Vieira, C.S., Pereira, P.M., 2015. Use of recycled construction and demolition materials in geotechnical applications: A review. Resour. Conserv. Recycl. 103, 192–204. https://doi.org/10.1016/j.resconrec.2015.07.023.

Vieira, J., Senff, L., Gonçalves, H., Silva, L., Ferreira, V.M., Labrincha, J.A., 2014. Functionalization of mortars for controlling the indoor ambient of buildings. Energy Build. 70, 224–236. https://doi.org/10.1016/j.enbuild.2013.11.064.

Vieira, T., Alves, A., de Brito, J., Correia, J.R., Silva, R.V., 2016. Durability-related performance of concrete containing fine recycled aggregates from crushed bricks and sanitary ware. Mater. Des. 90, 767–776. https://doi.org/10.1016/j.matdes.2015.11.023.

Villoria Saez, P., Del Rio Merino, M., Porras Amores, C., San Antonio Gonzalez, A., 2011. European Legislation and Implementation Measures

in the Management of Construction and Demolition Waste. Open Constr. Build. Technol. J. 5, 156–161. https://doi.org/10.2174/1874836801105010156.

Wang, W.-C., Wang, H.-Y., Lo, M.-H., 2015. The fresh and engineering properties of alkali activated slag as a function of fly ash replacement and alkali concentration. Constr. Build. Mater. 84, 224–229. https://doi.org/10.1016/j.conbuildmat.2014.09.059.

Wang, Y., Du, T., Song, Y., Che, S., Fang, X., Zhou, L., 2017. Amine-functionalized mesoporous ZSM-5 zeolite adsorbents for carbon dioxide capture. Solid State Sci. 73, 27–35. https://doi.org/10.1016/j.solidstatesciences.2017.09.004.

Wen, N., Zhao, Y., Yu, Z., Liu, M., 2019. A sludge and modified rice husk ash-based geopolymer: synthesis and characterization analysis. J. Clean. Prod. 226, 805–814. https://doi.org/10.1016/j.jclepro.2019.04.045.

Weng, L., Sagoe-Crentsil, K., 2007. Dissolution processes, hydrolysis and condensation reactions during geopolymer synthesis: Part I—Low Si/Al ratio systems. J. Mater. Sci. 42, 2997–3006. https://doi.org/10.1007/s10853-006-0820-2.

Xie, J., Kayali, O., 2014. Effect of initial water content and curing moisture conditions on the development of fly ash-based geopolymers in heat and ambient temperature. Constr. Build. Mater. 67, 20–28. https://doi.org/10.1016/j.conbuildmat.2013.10.047.

Yan, H., Xue-min, C., Jin, M., Liu, L., Liu, X., Chen, J., 2012. The hydrothermal transformation of solid geopolymers into zeolites. Microporous Mesoporous Mater. 161, 187–192. https://doi.org/10.1016/j.micromeso.2012.05.039.

Yip, C.K., Provis, J.L., Lukey, G.C., van Deventer, J.S.J., 2008. Carbonate mineral addition to metakaolin-based geopolymers. Cem. Concr. Compos. 30, 979–985. https://doi.org/10.1016/j.cemconcomp.2008.07.004.

Zaharaki, D., Galetakis, M., Komnitsas, K., 2016. Valorization of construction and demolition (C&D) and industrial wastes through alkali activation. Constr. Build. Mater. 121, 686–693. https://doi.org/10.1016/j.conbuildmat.2016.06.051.

Zhang, H., Yoshino, H., Hasegawa, K., Liu, J., Zhang, W., Xuan, H.,

2017. Practical moisture buffering effect of three hygroscopic materials in real-world conditions. Energy Build. 139, 214–223. https://doi.org/10.1016/j.enbuild.2017.01.021.

Zhang, M., El-Korchi, T., Zhang, G., Liang, J., Tao, M., 2014. Synthesis factors affecting mechanical properties, microstructure, and chemical composition of red mud–fly ash based geopolymers. Fuel 134, 315–325. https://doi.org/10.1016/j.fuel.2014.05.058.

Zhang, Z., Li, L., He, D., Ma, X., Yan, C., Wang, H., 2016. Novel self-supporting zeolitic block with tunable porosity and crystallinity for water treatment. Mater. Lett. 178, 151–154. https://doi.org/10.1016/j.matlet.2016.04.214.

Zhang, Z., Provis, J.L., Reid, A., Wang, H., 2014. Fly ash-based geopolymers: The relationship between composition, pore structure and efflorescence. Cem. Concr. Res. 64, 30–41. https://doi.org/10.1016/j.cemconres.2014.06.004.

Zheng, Z., Ma, X., Zhang, Z., Li, Y., 2019. In-situ transition of amorphous gels to Na-P1 zeolite in geopolymer: Mechanical and adsorption properties. Constr. Build. Mater. 202, 851–860. https://doi.org/10.1016/j.conbuildmat.2019.01.067.

Zhuang, X.Y., Chen, L., Komarneni, S., Zhou, C.H., Tong, D.S., Yang, H.M., Yu, W.H., Wang, H., 2016. Fly ash-based geopolymer: clean production, properties and applications. J. Clean. Prod. 125, 253–267. https://doi.org/10.1016/j.jclepro.2016.03.019.

Zribi, M., Samet, B., Baklouti, S., 2019. Effect of curing temperature on the synthesis, structure and mechanical properties of phosphate-based geopolymers. J. Non. Cryst. Solids 511, 62–67. https://doi.org/10.1016/j.jnoncrysol.2019.01.032.